Dispersion and attenuation relations in Flexoelectricity

Antonios E. Giannakopoulos[1] and Ares J. Rosakis[2]

[1]*Mechanics Division, National Technical University of Athens, Greece*

[2]*Graduate Aerospace Laboratory, California Institute of Technology, Pasadena CA 91125 (CA) USA*

Abstract

The dispersion relations in flexoelectricity are examined for plane time-harmonic waves that propagate in the flexoelectric materials. In contrast to classic elastodynamics, dispersion is observed in the displacement field due to two micro-structural and two micro-inertial lengths that emerge from the electromechanical coupling. In the absence of such coupling we return to the classic elastodynamic results. The problem dissociates in longitudinal and transverse waves, as is the case in classic elastodynamics. The group velocity of the mechanical field is also the velocity of the energy transfer across the planes of the waves. An optical branch of the dispersion relation appears due to the polarization field that follows the mechanical field. The longitudinal and transverse velocities of the plane waves was found to depend on the corresponding microstructural lengths and are less than or equal to the classic plane wave velocities because the micro-inertial lengths are greater than or equal to the micro-structural length. The opposite effect is expected when we encounter flexoelectric metamaterials in which case the micro-inertial lengths are less than the micro-structural length.

Key words: flexoelectricity, plane waves, dispersion curves, flexoelectric metamaterials

1. Introduction

Flexoelectricity is the ability of materials to convert mechanical strain gradients to electric polarization and vice versa. However, an electric field that changes with time gives rise to a magnetic field that has to be accounted for. Many rocks that consist earth's mantle exhibit flexoelectricity, often combined with piezoelectricity (in case of anisotropy). An excellent recent perspective of this unusual electromechanical coupling with emphasis on applications in energy harvesting, micro-electro-mechanical systems, nanotechnology and biology can be found in **Krichen and Sharma**

(2016) as well as other review articles like **Tagantsev (1991), Yudin and Tagantsev (2013)**, **Zubko et al. (2013)**, **Wang et al (2019)** to mention but few.

Flexoelectricity is considered to be the only source of strain gradient effects, and the coupling of the mechanical problem is analogous to a problem of couple stress elasticity where the two characteristic types of lengths emerge as a combination of mechanical, dielectric and flexoelectric constants, **Giannakopoulos and Rozakis (2020)**. The first type of length resembles the (well known in the context of couple stress elasticity) microstructural length which is connected to the displacement curvature (see also the anti-plane problem in static form by **Gavardinas et al, 2018** and in dynamic form by **Giannakopoulos and Zisis, 2019)**. The second type of length is less referenced (and hardly considered in metrology) and resembles the microinertial length that essentially introduces a non-classic kinetic energy term that connects to the micro-rotations of the matter. As will be shown, these micro-lengths create dispersion of plane waves, in contrast with classic elasto-dynamics that predict no such dispersion. Therefore, these dispersion relations are fundamentally different than the geometrically related dispersion encountered in wave guides such as circular cylinder, plates etc that show dispersion in the context of classical elastodynamics (see for example **Achenbach (1990), Bleustein and Stanley (1970), Mindlin and McNiven (1960), Pochhammer (1886)**). Recently, dispersion analyses of flexoelectric wave guides have been conducted for extension of rods, **Qu et al (2021a)**, and for torsion of rectangular rods, **Qu et al (2021b)**.

The paper is structured as follows. Section 2 provides the basic mechanical and electromagnetic field equations and corresponding boundary conditions. Section 3 performs the dispersion analysis for the mechanical and the optical cases separately, giving the corresponding dispersion relations between the frequency and the wave numbers. The phase velocities and the group velocities are found in closed forms. The group velocities are shown to be energy transport velocities in the Appendix. Section 4 gives the wave numbers as functions of the frequency. The analysis shows that two of the four wavenumbers of the dispersion analysis are imaginary. Section 5 provides the comparison with available experimental results. Section 5 gives the analysis of plane waves in an infinite flexoelectric body. Section 7 gives a brief account of flexoelectric metamaterials and the analogy with viscoelasticity. Finally, Section 8 concludes with basic findings of the work.

2. Flexoelectricity: The mechanical and the electromagnetic fields

We examine a homogeneous linear flexoelectric solid (being dielectric at the same time) with an energy density due to elastic deformation and electric polarization which depends on the strain gradients. Reverse flexoelectricity implies that the gradient of the polarization produces strain and should be included in the energy density. The elastic strain energy due to strain gradient effects will not be considered and the kinetic strain energy will not include micro-rotational effects.

In what follows, consider the flexo-electric problem with key unknowns the displacement vector [m], the polarization vector [C/m^2] and the electric field vector [N/C]. These are functions of the Cartesian coordinates x_i, and the time t. To clarify the new statement of the problem, we will follow the approach of **Giannakopoulos and Rosakis (2020)** and decouple the problem to one that involves only the displacement vector (dynamic equation) and another that involves the polarization vector in relation to the displacement (transfer equation).

In what follows, consider the flexo-electric problem with key unknowns the material displacement vector u_i [m], the material (electric) polarization vector P_i [C/m^2] and the electric field E_i [Nm/C]. These are functions of the (right-handed) Cartesian coordinates x_1, x_2, x_3 and the time t. The linear internal energy density function that includes deformation and polarization is (**Mindlin, 1968; Maraganti et al, 2006; Hu et al, 2017**):

$$W = \left[\begin{array}{l} \frac{1}{2} a_{ij} P_i P_j + \frac{1}{2} b_{ijkl} P_{j,i} P_{l,k} + \frac{1}{2} c_{ijkl} \varepsilon_{ij} \varepsilon_{kl} + e_{ijkl} P_{j,i} \varepsilon_{kl} \\ \qquad + f_{ijkl} P_i \varepsilon_{kl,j} + b^0_{ij} P_{j,i} \end{array} \right] \tag{2.1}$$

The mechanical linear strain is related to the displacement vector as $\varepsilon_{ij} = (u_{i,j} + u_{j,i})/2$. $P_{i,j}$ is the gradient of the polarization vector P_i and $\varepsilon_{ij,k}$ are the gradients of the strains. Repeated indices imply summation from 1 to 3 and $(\ )_{,i} = \partial / \partial x_i$. The dielectric body will be assumed to be a perfect insulator, so the gradient of the polarization vector is minus the bounded charge inside the body, $\nabla \cdot \vec{P} = -\rho_{bound}$ [C/m^3]. The compatibility equations are identical to classic linear elasticity. The form of the energy density function (2.1) omits an extra term that ensures thermodynamic stability of the total energy ($1/2 g_{ijklmn}\, u_{i,jk}\, u_{l,mn}$). This term represents the contribution of purely elastic nonlocal effects. This energy addition may stabilize the problems in case that the microstructural lengths ℓ_p, ℓ_s defined below in eqs. (2.30) and (2.31) are not real and positive, something that has not been experimentally observed so far.

It has been found however (see **Maraganti et al (2006), erratum**) that, for most problems, excluding this contribution is generally small, although, if flexoelectricity is incorporated, it is required to guarantee thermodynamic stability. For some problems, this omission (or inclusion) of this term may be important especially where stability is an issue.

The material constants are: the elastic constant tensor c_{ijkl} [N/m^2], the flexo-electric coefficient tensor f_{ijkl} [Nm/C], the reciprocal dielectric susceptibility tensor a_{ij} [Nm^2/C^2], the inverse flexo-electric coefficient tensor e_{ijkl} [Nm/C] and the gradient polarization coupling tensor b_{ijkl} [Nm^4/C^2]. The symmetries of the above constants have been addressed in **Shu et al (2011)**. All these material tensors should be positive definite. The constants b_{ij}^0 are related to the surface energy per unit area $T_s = (n_l b_{ij}^0 P_j)/2$ with n_i being the unit normal vector pointing outside the flexoelectric body (**Mindlin, 1968**) and do not affect the balance laws, but only the boundary conditions.

In the works on continuum flexoelectricity so far, the Maxwell electric self-field E_i was stated by an electric potential as $E_i = -\Phi_{,i}$ [N/C]. In this work, and in anticipation of the interaction with the magnetic field, we leave the electric field to be general. The total electric enthalpy is (**Toupin, 1956**):

$$\bar{H} = W - \frac{1}{2}\varepsilon_0 E_i E_i - E_i P_i \tag{2.2}$$

where, $\varepsilon_0 \approx 8.854\times10^{-12} C^2 N^{-1} m^{-2} [= \mathrm{Fm}^{-1}]$ is the dielectric permittivity of vacuum (assumed to surround the body).

The kinetic energy density is:

$$T = \frac{1}{2}\rho \dot{u}_3 \dot{u}_3 \tag{2.3}$$

where ρ is the material mass density and $\dot{u}_i = \partial u_i / \partial t$ is the material velocity vector. If $\rho = 0$, the problem reduces to the static case.

Accordingly, the constitutive equations are written as:

a. Cauchy (symmetric) stress tensor:

$$\sigma_{ij} = \frac{\partial W}{\partial \varepsilon_{ij}} = c_{ijkl}\varepsilon_{kl} + e_{klij}P_{l,k} \tag{2.4}$$

b. Dipolar stress tensor:

$$\tau_{ijk} = \frac{\partial W}{\partial \varepsilon_{jk,i}} = f_{lijk}P_l \tag{2.5}$$

c. Effective local electric force:

$$\bar{E}_k = -\frac{\partial W}{\partial P_k} = -\left(a_{kj}P_j + f_{klij}\varepsilon_{ij,l}\right) \tag{2.6}$$

d. Polarization gradient force:

$$E_{ij} = \frac{\partial W}{\partial P_{j,i}} = b_{ijkl} P_{l,k} + e_{ijkl} \varepsilon_{kl} + b^0_{ij} \tag{2.7}$$

We will concentrate in the isotropic response and in this case the material tensors become

$$a_{ij} = a\delta_{ij} \tag{2.8}$$

$$c_{ijkl} = c_{12}\delta_{ij}\delta_{kl} + c_{44}(\delta_{ik}\delta_{jl} + \delta_{jk}\delta_{il}) \tag{2.9}$$

$$f_{ijkl} = f_{12}\delta_{ij}\delta_{kl} + f_{44}(\delta_{ik}\delta_{jl} + \delta_{jk}\delta_{il}) \tag{2.10}$$

$$e_{ijkl} = e_{12}\delta_{ij}\delta_{kl} + e_{44}(\delta_{ik}\delta_{jl} + \delta_{jk}\delta_{il}) \tag{2.11}$$

$$b_{ijkl} = b_{12}\delta_{ij}\delta_{kl} + b_{44}(\delta_{ik}\delta_{jl} + \delta_{jk}\delta_{il}) + b_{77}(\delta_{ik}\delta_{jl} - \delta_{jk}\delta_{il}) \tag{2.12}$$

$$b^0_{ij} = b_0\delta_{ij} \tag{2.13}$$

where δ_{ij} is Kronecker's delta (identity tensor). All material constants are positive definite and bounded. The dielectric susceptibility χ relates to the dielectric constant of vacuum ε_0 as $1/a = \chi\varepsilon_0$. The classic elastic dielectric case is obtained, if $f_{ijkl} = 0$ and $e_{ijkl} = 0$, whereas the classic elastic case requires additionally $a_{ij} = 0$ and $b^0_{ij} = 0$. If only $f_{ijkl} = 0$, we recover the formulation of **Mindlin (1968; 1969)** for a dielectric solid with polarization gradient.

Using Hamilton's principle (least action), that is minimization of the total electric enthalpy with respect to u_i and P_i in the whole body volume V and arbitrary time interval $(0, t_1)$,

$$\int_0^{t_2}\int_V \delta(\bar{H} - T)dVdt = 0 \tag{2.14}$$

we obtain the Euler conditions for all the material points of the body (in the presence of body forces X_i [N/m^3] and initial electric field E^0_i [N/C]):

a. Conservation of linear momentum:

$$\sigma_{ji,j} - \tau_{kji,jk} + X_i = \rho\ddot{u}_i \tag{2.15}$$

b. Conservation of electric field:

$$\bar{E}_j + E_{ij,i} + E_j + E^0_j = 0 \tag{2.16}$$

Note that in right hand side of eq. (2.16) the polarization inertia $d_0\ddot{\dot{P}}$ is considered to be negligible.

c. Gauss' law (absence of free charges) inside the body:

$$D_{i,i} = \varepsilon_0 E_{i,i} + P_{i,i} = 0 \tag{2.17}$$

where $D_i = \varepsilon_0 E_i + P_i$ is the electric displacement.

d. Maxwell-Faraday equations outside the body (in absence of magnetic flux):

$$\nabla \times \vec{E} = \vec{0} \tag{2.18}$$

where ∇ is the gradient operator,or, using the alternating Levi-Civita tensor, $\varepsilon_{ijk} E_{k,j} = 0$. The corresponding, work conjugate, boundary conditions are summarized in Table 1. The electric boundary conditions can be materialized with appropriate steady state currents applied by surface conductors, **Jackson (1975)**. In the present approach, the Maxwell electromagnetic stresses $D_j \overline{E}_i - (\mathrm{D}_k \overline{\mathrm{E}}_k)\delta_{ij} / 2$ are considered much smaller than the mechanical stresses σ_{ij} . For a thorough discussion of the influence of Maxwell and electrostatic stresses in flexoelectricity refer to **Hu and Shen (2010)**.

Table 1: Mutually exclusive boundary conditions for the flexoelectric problem.

Mutually Exclusive Boundary Conditions	
Essential Boundary Conditions	**Dynamic Boundary Conditions**
P_i	$n_j E_{ji}$
Φ	$n_i \left(\varepsilon_0 \left\| E_i \right\| - \left\| P_i \right\| \right) = \sigma_s$
Du_i	$r_i = \tau_{kji} n_k n_j$
u_i	$t_i = \sigma_{ij} n_j - \tau_{kji,k} n_j + (D_l n_l) n_j n_k \tau_{kji} - D_j (\tau_{kji} n_k)$

n_i is the unit normal vector pointing outside the body
$D \equiv n_k \partial / \partial x_k$ is the normal to the surface derivative
$D_j \equiv (\delta_{jk} - n_j n_k)\partial / \partial x_k$ is the tangential to the surface derivative
$\| \| = (\ )^+ - (\ )^-$ is the jump from outside of the body (+) to the inside of the body (-)
σ_s is the surface charge imposed on the dielectric boundary

The initial conditions are

$$u_i(\vec{x},0) = u_i^0(\vec{x})$$

$$\dot{u}_i(\vec{x},0) = \dot{u}_i^0(\vec{x}) \qquad (2.19)$$

$$P_i(\vec{x},0) = P_i^0(\vec{x})$$

where u_i^0 is the initial displacement vector, $\dot{u}_i^0$ is the initial velocity vector and P_i^0 is the initial polarization vector. The initial fields are considered to be known and are often taken to be zero.

Furthermore, assuming zero body forces and initial electric field ($X_i = 0[\mathrm{N/m^3}]$, $E_i^0 = 0[\mathrm{N/C}]$), we transform Eqs. (2.15) and (2.16) into Navier-type of equations:

$$c_{44}\nabla^2 u_i + (c_{12} + c_{44})\nabla_i(\nabla_k u_k) + (e_{44} - f_{12})\nabla^2 P_i + (e_{12} + e_{44} - 2f_{44})\nabla_i(\nabla_k P_k) = \rho\ddot{u}_i \qquad (2.20)$$

$$\begin{aligned}&(e_{44} - f_{12})\nabla^2 u_i + (d_{12} + d_{44} - 2f_{44})\nabla_i(\nabla_k u_k) + (b_{44} + b_{77})\nabla^2 P_i + (b_{12} + b_{44} - b_{77})\nabla_i(\nabla_k P_k) \\ &-aP_i + E_i = 0\end{aligned} \qquad (2.21)$$

where, $\nabla^2 = \nabla_k \nabla_k = \partial^2/\partial x_1^2 + \partial^2/\partial x_2^2 + \partial^2/\partial x_3^2$ is the Laplacian operator, $\nabla^4 = \nabla^2\nabla^2$ is the biharmonic operator. Note that, if $f_{ijkl} = 0$, $e_{ijkl} = 0$ and $a_{ij} = 0$, we obtain from (2.20) the classic elastodynamic equations and (2.21) is identically zero.

Starting from the Navier-type of equations (2.21), we take the gradient on (2.21) and on (2.17) and eliminate the electric field to obtain:

$$\begin{aligned}&(e_{44} - f_{12})\nabla\cdot\nabla^2\vec{u} + (e_{12} + e_{44} - 2f_{44})\nabla^2\nabla\cdot\vec{u} \\ &+(b_{44} + b_{77})\nabla\cdot\nabla^2\vec{P} + (b_{12} + b_{44} - b_{77})\nabla^2\nabla\cdot\vec{P} - (a + \varepsilon_0^{-1})\nabla^2\nabla\cdot\vec{P} = 0\end{aligned} \qquad (2.22)$$

Thus the reformulation of the problem leads to solving two coupled equations (2.20) and (2.22) with respect to the displacement vector u_i and the polarization vector P_i.

The representation of the general solution of (2.20), (2.22) has been given by **Giannakopoulos and Rosakis (2020)** as a Helmholtz decomposition of both the displacement and the polarization vectors as

$$\vec{u} = \nabla\phi + \nabla\times\vec{H}^* \qquad \nabla\cdot\vec{H}^* = 0 \tag{2.23}$$

$$\vec{P} = \nabla\chi^* + \nabla\times\vec{\mathrm{K}} \qquad \nabla\cdot\vec{K} = 0 \tag{2.24}$$

where $\phi(\vec{x},t)$ and $\chi^*(\vec{x},t)$ are scalar functions, whereas $\vec{H}^*(\vec{x},t)$ and $\vec{K}(\vec{x},t)$ are vector functions that are solutions of

$$\nabla^2\phi - \ell_p^2\nabla^4\phi = \frac{1}{c_p^2}\left(\ddot{\phi} - h_p^2\nabla^2\ddot{\phi}\right) \tag{2.25}$$

$$\nabla^2\vec{H}^* - \ell_s^2\nabla^4\vec{H}^* = \frac{1}{c_s^2}\left(\ddot{\vec{H}}^* - h_s^2\nabla^2\ddot{\vec{H}}^*\right) \tag{2.26}$$

$$\nabla^2\chi^* - \ell_p^2\nabla^4\chi^* = \frac{1}{c_p^2}\left(\frac{e_{11}-f_{11}}{a+\varepsilon_0^{-1}}\nabla^2\ddot{\phi}\right) \tag{2.27}$$

$$\nabla^2\vec{K} - \ell_s^2\nabla^4\vec{K} = \frac{1}{c_s^2}\left(\frac{e_{44}-f_{12}}{a}\nabla^2\ddot{\vec{H}}^*\right) \tag{2.28}$$

where the characteristic dilatation and shear speeds appear as in the classic elastodynamics

$$\begin{aligned} c_p &= \sqrt{\frac{c_{11}}{\rho}} = \sqrt{\frac{c_{12}+2c_{44}}{\rho}} = \sqrt{\frac{\lambda+2\mu}{\rho}} = \sqrt{\frac{E(1-\nu)}{\rho(1+\nu)(1-2\nu)}} \\ c_s &= \sqrt{\frac{c_{44}}{\rho}} = \sqrt{\frac{\mu}{\rho}} = \sqrt{\frac{E}{2\rho(1+\nu)}} < c_p \end{aligned} \tag{2.29}$$

where E, and ν are the Young's modulus and the Poisson's ratio respectively, and (λ,μ) are the classic Lame constants. Moreover, in the above equations four lengths appear, defined by

$$\left\{\mu, a, f_{12}, f_{44}, e_{44}, b_{44}+b_{77}, \mu\left(b_{44}+b_{77}\right)-e_{44}^2\right\} > 0$$

$$\ell_s^2 = \frac{b_{44}+b_{77}}{a} - \frac{\left(e_{44}-f_{12}\right)^2}{\mu a} \geq 0 \tag{2.30}$$

$$h_s^2 = \frac{\left(b_{44}+b_{77}\right)}{a} \geq \ell_s^2 \geq 0$$

$$\left\{b_{11}=b_{12}+2b_{44}, a,\ f_{11}=f_{12}+2f_{44}, e_{11}=e_{12}+2e_{44},\ f_{44}, (\lambda+2\mu)b_{11}-e_{11}^2\right\}>0$$

$$\ell_p^2=\frac{b_{11}}{a+\varepsilon_0^{-1}}-\frac{\left(e_{11}-f_{11}\right)^2}{(\lambda+2\mu)(a+\varepsilon_0^{-1})}\geq 0 \tag{2.31}$$

$$h_p^2=\frac{b_{11}}{a+\varepsilon_0^{-1}}\geq \ell_p^2\geq 0$$

Thus, we obtain two "micro-structural" related lengths (ℓ_p,ℓ_s) and two "micro-inertial" related lengths (h_p,h_s). Note that the positive ness of the lengths stems from the assumed convexity of the energy density. Gradient dielectricity also yields the internal lengths (ℓ_p,ℓ_s) and (h_p,h_s) while, flexo-electricity leads to higher microstructural lengths, compared to gradient dielectricity. The mechanical response is similar to the Mindlin's model of linear elastic solids with microstructure (**Mindlin, 1963**). We further note that polarization exhibits a size effect similar to the size effect of the mechanical displacement. The body forces and the initial electric fields may be easily incorporated in eqs. (2.25-2.28) provided we can represent these fields as the displacement and polarization field in eqs. (2.23) and (2.24).

Typical material constants for PMMA (poly-methyl-methacrtylate) were estimated and are shown in Table 2 and are obtained from **Giannakopoulos and Rozakis (2020)**. A rather complete material data for alkali halides have been found by **Askar et al (1970)** and are also summarized in **Table 2**.

Table 2: Typical material constants.

Constant	**Units**	NaI	KI	NaCl	KCl	PMMA
$\mu=c_{44}$	*GPa*	7.2	4.4	12.8	6.8	2.215
$\lambda+2\mu=c_{12}+2c_{44}$	*GPa*	21.4	12.7	38.4	19.9	9.585
$/e_{44}-f_{12}/$	*Nm/C=V*	-2.10	-1.94	-2.42	-2.15	7.015
$/e_{11}-f_{11}/$	*Nm/C=V*	3.81	3.42	4.67	3.92	56.12

b_{11}	Nm^4/C^2	$0.712\ 10^{-9}$	$1.110\ 10^{-9}$	$0.688\ 10^{-9}$	$1.20\ 10^{-9}$	$1.807\ 10^{-6}$
$(b_{44}+b_{77})$	Nm^4/C^2	$0.712\ 10^{-9}$	$1.110\ 10^{-9}$	$0.688\ 10^{-9}$	$1.20\ 10^{-9}$	$1.807\ 10^{-6}$
a	Nm^2/C^2	$137\ 10^8$	$176\ 10^8$	$174\ 10^8$	$243\ 10^8$	$6.275\ 10^{10}$
ρ	kg/m^3	3670	3120	2160	1980	1180
c_s	m/s	1401	1188	2434	1853	1370
c_p	m/s	2415	1994	4216	3170	2850
ℓ_p	nm	0.00179	0.00821	0.0664	0.01887	2.9
h_p	nm	0.07498	0.09221	0.07265	0.09351	3.2075
ℓ_s	nm	0.0166	0.0306	0.0376	0.0549	4.521
h_s	nm	0.2280	0.2511	0.1988	0.2222	4.535
a_0 Atomic radius	nm	0.323	0.353	0.281	0.314	
Ω_p	THz	33	26	50	40	
Ω_s	THz	22	19	31	27	
$-b^0$	Nm/C	$1.26\ 10^{-2}$	$1.15\ 10^{-2}$	$1.44\ 10^{-2}$	$1.29\ 10^{-2}$	
$\varepsilon_0 = 1/(36\pi) \times 10^{-9} \approx 8.854 \times 10^{-12}\ C^2\ N^{-1}\ m^{-2}$ dielectric constant at vacuum						

The general solution starts from the mechanical response, solving (2.25) for $\phi(\vec{x},t)$, and (2.26) for $\vec{H}^*(\vec{x},t)$. Once the displacement vector is found, the polarization vector can be found from the solution of (2.27) for $\chi^*(\vec{x},t)$ and (2.28) for $\vec{K}(\vec{x},t)$.

3. The dispersion relations

The discrete atomic structure of crystals implies a dispersive medium, even in the absence of the flexoelectric effect **(Brillouin, 1946).** In the present case, the relation between the frequency $\omega/2\pi$ and the wave number k can be obtained from the dynamic equilibrium equations (2.25) for the dilatational waves, and (2.26) for the shear waves. Due to conservation of energy assumed in the present model, the frequency is real, whereas the wave number may be complex. The dynamic equation will provide two dispersion relations, as has been indicated by **Gouriotis and Georgiadis (2015)** for the Toupin-Mindlin gradient theory (with one micro-inertial length).

Assuming a solution of the type $\phi=\overline{\phi}\exp[-i\omega t]\exp[ik(\vec{n}\cdot\vec{x})]$, where $\vec{n}$ is the in-plane unit direction vector of travelling waves and $i=\sqrt{-1}$, and replacing this type of solution in (2.25), we obtain a dispersion relation for the dilatation mechanical wave as:

$$\omega^2=k^2c_p^2\frac{1+\ell_p^2k^2}{1+h_p^2k^2} \tag{3.1}$$

and the phase velocity reads as:

$$\left(\frac{\omega}{k}\right)_p=c_p\left(\frac{1+\ell_p^2k^2}{1+h_p^2k^2}\right)^{1/2}\le c_p \tag{3.2}$$

The dilatational energy propagates with group velocity $d\omega/dk$ which reads as:

$$\begin{aligned}&\left(\frac{d\omega}{dk}\right)_p=\left(\frac{\omega}{k}\right)_p+c_p\left(\ell_p^2k^2-h_p^2k^2\right)\left(1+\ell_p^2k^2\right)^{-1/2}\left(1+h_p^2k^2\right)^{-3/2}=\\&\left(\frac{\omega}{k}\right)_p\frac{1+k^2\ell_p^2}{1+k^2h_p^2}=\left(\frac{\omega}{k}\right)_p^3\frac{1}{c_p^2}\le\left(\frac{\omega}{k}\right)_p\end{aligned} \tag{3.3}$$

So the group velocity is less than the phase velocity, because $h_p^2\ge\ell_p^2$, and varies smoothly between the values:

$$k \to 0, \quad \left(\frac{d\omega}{dk}\right)_p = \left(\frac{\omega}{k}\right)_p = c_p \tag{3.4}$$

$$k \to \infty, \quad \left(\frac{d\omega}{dk}\right)_p = c_p \frac{\ell_p^2}{h_p^2} \le c_p \tag{3.5}$$

Note that for $h_p = \ell_p$ or $(h_p, \ell_p) \to 0$, the dilatational wave velocity degenerates into the non-dispersive velocity of classical elastodynamics. Assuming now a solution of the type $\vec{H}^* = \vec{\bar{H}}^* \exp[-i\omega t] \exp[ik(\vec{n} \cdot \vec{x})]$, where $\vec{n}$ is the in-plane unit direction vector of travelling waves, and replacing this type of solution in (2.26), we obtain a dispersion relation for the shear mechanical wave as:

$$\omega^2 = k^2 c_s^2 \frac{1 + \ell_s^2 k^2}{1 + h_s^2 k^2} \tag{3.6}$$

and the phase velocity reads as:

$$\left(\frac{\omega}{k}\right)_s = c_s \left(\frac{1 + \ell_s^2 k^2}{1 + h_s^2 k^2}\right)^{1/2} \tag{3.7}$$

The dilatational energy propagates with group velocity which reads as:

$$\begin{aligned} &\left(\frac{d\omega}{dk}\right)_s = \left(\frac{\omega}{k}\right)_s + c_s \left(\ell_s^2 k^2 - h_s^2 k^2\right)\left(1 + \ell_s^2 k^2\right)^{-1/2} \left(1 + h_s^2 k^2\right)^{-3/2} = \\ &\left(\frac{\omega}{k}\right)_s \frac{1 + k^2 \ell_s^2}{1 + k^2 h_s^2} = \left(\frac{\omega}{k}\right)_p^3 \frac{1}{c_p^2} \le \left(\frac{\omega}{k}\right)_s \end{aligned} \tag{3.8}$$

Note that for $h_s = \ell_s$ or $(h_s, \ell_s) \to 0$, the shear wave velocity degenerates into the non-dispersive velocity of classical elastodynamics. As for the dilatational waves, the group velocity for the shear waves is less than their phase velocity and varies smoothly between the values:

$$k \to 0, \quad \left(\frac{d\omega}{dk}\right)_s = \left(\frac{\omega}{k}\right)_s = c_s \tag{3.9}$$

$$k \to \infty, \quad \left(\frac{d\omega}{dk}\right)_s = c_s \frac{\ell_s^2}{h_s^2} \le c_s \tag{3.10}$$

Dispersion is due to the ratio of the micro-structural to the micro-inertial lengths. If these ratios are one, we return to the classic non-dispersive case. Our analysis predicts that the micro-inertia lengths have an important effect at high frequencies with wave lengths that are comparable with the micro-structural length. Comparing the phase velocities, we observe that

$$\left(\frac{c_p}{c_s}\right)^2 \geq \frac{b_{44}+b_{77}}{b_{11}} \Leftrightarrow \left(\frac{\omega}{k}\right)_p \geq \left(\frac{\omega}{k}\right)_s \text{ and } \left(\frac{d\omega}{dk}\right)_p \geq \left(\frac{d\omega}{dk}\right)_s \tag{3.11}$$

Indeed, the known material parameters indicated that the ratio $\left(b_{44}+b_{77}\right)/b_{11}$ is never larger than 2 and c_p^2/c_s^2 is not smaller than 2 (see for example **Table 2**). Nevertheless, condition (3.11) does not stem from any theory and should not be taken for granted for all natural and synthetic dielectric materials. Condition (3.11) is also necessary and sufficient for a similar inequality for the group velocity.

Assuming $\phi = \overline{\phi}\exp[-i\omega t]\exp[ik(\vec{\mathrm{n}}\cdot\vec{\mathrm{x}})]$ and $\chi^* = S_p\overline{\phi}\exp[-i\omega t]\exp[ik(\vec{\mathrm{n}}\cdot\vec{\mathrm{x}})]$, the transfer equation (2.27) provides a "dispersion-like" relation which we will accept as a soft-mode optical dispersion related to the dilatational mechanical waves

$$\omega^2 = c_p^2\frac{-\left(a+\varepsilon_0^{-1}\right)}{e_{11}-f_{11}}S_p\left[1+\ell_p^2k^2\right] \tag{3.12}$$

For real frequencies, we must have $-\left(a+\varepsilon_0^{-1}\right)S_p/(e_{11}-f_{11})>0$ and the two fields must be in phase. Interestingly, **Huller (1969)**, using lattice dynamics and the quantum result of **Barrett (1952)** provides a soft-mode optical dispersion relation for perovskites of the type:

$$\omega^2 \approx \Omega_p^2 + \Lambda_p k^2 \tag{3.13}$$

In (3.13), Ω_p is a frequency at zero wave number (cut-off frequency) that is inversely proportional to the dielectric constant (or proportional to a in our presentation). The dielectric constant depends critically on the temperature, **Barrett (1952).** Comparing (3.12) and (3.13) we can identify Huller's parameters as

$$\Omega_p^2 = \frac{-\left(a+\varepsilon_0^{-1}\right)}{e_{11}-f_{11}}S_pc_p^2 \tag{3.14}$$

$$\Lambda_p = \Omega_p^2 \ell_p^2 \tag{3.15}$$

Next, assuming $\vec{H}^* = \vec{\bar{H}}^* \exp[-i\omega t]\exp[ik(\vec{n}\cdot\vec{x})]$ and $\vec{K} = S_s \vec{\bar{K}} \exp[-i\omega t]\exp[ik(\vec{n}\cdot\vec{x})]$, the transfer equation (2.28) provides a "dispersion-like" relation which we will accept as a soft-mode optical dispersion related to the shear mechanical waves

$$\omega^2 = c_s^2 \frac{-a}{e_{44} - f_{44}} S_s \left[1 + \ell_s^2 k^2\right] \tag{3.16}$$

For real frequencies, we must have $-aS_s / (e_{44} - f_{12}) > 0$ and the two field must be in-phase. Following **Huller (1969)**, the soft-mode optical dispersion relation related to shear type of mechanical waves is of the form:

$$\omega^2 \approx \Omega_s^2 + \Lambda_s k^2 \tag{3.17}$$

In (3.17), Ω_s is a frequency at zero wave number that is inversely proportional to the dielectric constant (or proportional to a in our presentation). The dielectric constant depends critically on the temperature, **Barrett (1952).** Comparing (3.16) and (3.17) we can identify Huller's parameters as

$$\Omega_s^2 = \frac{-a}{e_{44} - f_{44}} S_s c_s^2 \tag{3.18}$$

$$\Lambda_s = \Omega_s^2 \ell_s^2 \tag{3.19}$$

Values of Ω_p, Ω_s can be found in several books, e.g. **Kittel (1971)**.

It is interesting to note that in case $\ell_{p,s} \approx 0$ (semiconductors), the above dispersion relations take the general form (disregard indices p and s for shortness)

$$\omega^2 = k^2 c^2 \frac{1}{1 + h^2 k^2} \tag{3.20}$$

for the mechanical response and

$$\omega^2 \approx \Omega^2 \tag{3.21}$$

for the optical branch of the dispersion relation.

Figure 1a shows the normalized plot of the mechanical modes, implied by eqs. (3.1) and (3.6). **Figure 1b** shows the normalized plot of the optical modes, implied by eqs. (3.12) and (3.14). The normalized wave number is $\bar{\mathrm{k}} = \mathrm{k}h_{p,s}$. The suffix p,s denotes dilatational and shear part accordingly. The normalized frequency for the mechanical modes is $\bar{\omega} = \omega h_{p,s} / c_{p,s}$. The normalized frequency for the optical modes is $\bar{\omega} = \omega / \Omega_{p,s}$.

The normalized dispersion equations take the form

$$\boxed{\bar{\omega} = \bar{k}\left(\frac{1+(\ell_{p,s}/h_{p,s})^2\bar{k}^2}{1+\bar{k}^2}\right)^{1/2}} \tag{3.22}$$

for the mechanical modes and

$$\boxed{\bar{\omega} = \left[1+(\ell_{p,s}/h_{p,s})^2\bar{k}^2\right]^{1/2}} \tag{3.23}$$

for the optical modes. **Figure 2a** shows the normalized mechanical phase velocities $\bar{\omega}/\bar{k}$, as a function of the normalized wave number $\bar{k}$. Then, from (3.2) and (3.7), we obtain:

$$\boxed{\frac{\bar{\omega}}{\bar{k}} = \left(\frac{1+(\ell_{p,s}/h_{p,s})^2\bar{k}^2}{1+\bar{k}^2}\right)^{1/2}} \tag{3.24}$$

Figure 2b shows the normalized optical phase velocity $\bar{\omega}/\bar{k}$, as a function of the normalized wave number $\bar{k}$. Then, from (3.23), we obtain:

$$\boxed{\frac{\bar{\omega}}{\bar{k}} = \frac{1}{\bar{k}}\left[1+(\ell_{p,s}/h_{p,s})^2\bar{k}^2\right]^{1/2}} \tag{3.25}$$

Figure 3a shows the normalized mechanical group velocities $d\bar{\omega}/\mathrm{d}\bar{\mathrm{k}}$, as a function of the normalized wave number $\bar{k}$. Then, from (3.3) and (3.8), we obtain:

$$\boxed{\frac{d\bar{\omega}}{d\bar{k}} = \frac{\bar{\omega}}{\bar{k}} + \left(\left(\ell_{p,s}/h_{p,s}\right)^2\bar{k}^2 - \bar{k}^2\right)\left(1+\left(\ell_{p,s}/h_{p,s}\right)^2\bar{k}^2\right)^{-1/2}\left(1+\bar{k}^2\right)^{-3/2}} \tag{3.26}$$

In the **Appendix** we show that the mechanical group velocities (3.26) are the velocities of the transfer of the time average of the power per unit area to the twice the time average of the kinetic

energy across the plane of a time-harmonic plane wave (longitudinal and transverse) that travel inside the body.

Figure 3b shows the normalized optical group velocities $d\bar{\omega}/d\bar{k}$, as a function of the normalized wave number $\bar{k}$. Then, from (3.23), we obtain:

$$\boxed{\frac{d\bar{\omega}}{d\bar{k}} = \left(\ell_{p,s}/h_{p,s}\right)^2 \bar{k}\left(1+\left(\ell_{p,s}/h_{p,s}\right)^2 \bar{k}^2\right)^{-1/2}} \tag{3.27}$$

In these figures, there is a free parameter in the range $0 \le \ell_{p,s}/h_{p,s} \le 1$. As this parameter increases from 0 to 1, the mechanical dispersion relations start with the same slope at low frequencies and attain a linear asymptote at high frequencies, proportional to $\ell_{p,s}/h_{p,s}$. The optical dispersion relationships start at a high initial frequency and also attain a linear asymptote at high frequencies, proportional to $\ell_{p,s}/h_{p,s}$. Note that the optical frequencies are greater than the mechanical frequencies. The normalized phase and group velocities approach the value $\ell_{p,s}/h_{p,s}$ at high wave numbers $\bar{k} \to \infty$. The phase velocities are greater than the group velocities. The mechanical phase velocity, the mechanical group velocity and the optical group velocities have an upper bound of 1. The optical phase velocities are unbounded for small wave numbers $\bar{k} \to 0$. Note that the dilatation group velocity is greater than the shear group velocity for both the mechanical and the optical modes.

The derived dispersion relation (3.20) can be also related to the bond charge model of **Weber (1974)** that includes metal-like binding bonding by central forces between nearest-neighbor ions and covalent binding in interactions involving the bond actions, observed in many semiconducting material.

$$\frac{a_0^{\,2}}{4}\omega^2 = c^2 \frac{\sin^2(ka_0/2)}{1+2(f'/f)\sin^2(ka_0/2)} \tag{3.28}$$

where a_0 is the atomic cell dimension, and f'/f is the ratio of the ionic forces to the bond charge forces. The result holds for the Brillouin zone $0 \le ka_0/2 \le \pi/2$. For wave numbers less than $1/a_0$, the ratio of the internal lengths of the present theory indicates that the micro-structural length relates to the atomic cell dimension $a_0/2 = \ell$. The ratio of the ionic forces to the bond charge forces $(f'/f >> 1)$ can give an estimate of the ratio of the micro-inertial length to the micro-inertial length,

$$h=\frac{a_0}{2}\left(1+2\frac{f'}{f}\right)^{1/2} \tag{3.29}$$

The dispersion relations provide a good approximation to many experimental dispersion curves of flexoelectic materials. The comparisons include the dispersion of the transverse acoustic and soft optical results for $KTaO_3$ (potassium tantalite) found in the work of **Axe et al. (1970)**, for $PbTiO_3$ (lead titanate) by **Shirane et al. (1970)** and for $BaTiO_3$ (barium titanate) by **Harada et al. (1970)** and others. Examples of the above dispersion relations have been shown to fit well with experimental results for the shear type of waves, **Giannakopoulos and Zisis (2021)**.

It is of interest to point that the dispersion relation of the type (3.22) approximates the dispersion of the fundamental mode of a circular cylinder of radius R acting as a wave guide of longitudinal waves, **Achenbach (1990)**. In this case, an analogy can be established by assuming a micro-stuctural length and a micro-inertia length as

$$\begin{aligned}&\ell^2\to\frac{\nu R}{2}\\ &\frac{h^2}{\ell^2}\to\frac{0.862+1.14\nu}{1+\nu}\sqrt{2\left(1+\nu\right)}>1\end{aligned} \tag{3.30}$$

with a characteristic wave velocity

$$c\to\sqrt{\frac{E}{\rho}} \tag{3.31}$$

Another interesting analogy of the optical dispersion relation of the type (3.23) exist with the classic waveguides is the horizontally polarized shear waves propagating in an elastic layer of thickness 2H and is the first antisymmetric mode (n=1), **Achenbach (1990)**. In this case, an analogy can be established by assuming a micro-stuctural length as

$$\begin{aligned}&\ell^2\to\frac{2H}{\pi}\\ &\frac{h^2}{\ell^2}\to 0\end{aligned} \tag{3.32}$$

with a characteristic wave velocity

$$c_s = \sqrt{\frac{E}{2(1+\nu)\rho}} \tag{3.33}$$

and a cut-off frequency

$$\Omega_s \to \frac{\pi c_s}{2H} \tag{3.34}$$

4. Attenuation

Regarding the mechanical waves, solving (3.2) and (3.6) to express the wave number k as a function of the frequency $k(\omega)$, we obtain:

$$k_1^2(\omega) = \frac{2\omega^2}{c^2 - h^2\omega^2 + \sqrt{\left(c^2 - h^2\omega^2\right)^2 + 4\ell^2\omega^2c^2}} \geq 0 \tag{4.1}$$

and

$$k_2^2(\omega) = \frac{2\omega^2}{c^2 - h^2\omega^2 - \sqrt{\left(c^2 - h^2\omega^2\right)^2 + 4\ell^2\omega^2c^2}} < 0 \tag{4.2}$$

In the above results we have $\left\{c = c_p,\ \ \ell = \ell_p \neq 0,\ \ h = h_p\right\}$ for the dilatational waves and $\left\{c = c_s,\ \ \ell = \ell_s \neq 0,\ \ h = h_s\right\}$ for the transverse waves. These results imply that the k_1's are always real and the k_2's are always imaginary and $1/h < |k_1| < 1/\ell,\ \ |k_2| > |k_1|$. The imaginary wave numbers imply attenuated or evanescent waves (with zero cut-off frequency) that do not exist in classical elasto-dynamics $\left\{\ell = 0,\ \ h = 0,\ \ k_1^2 = \omega^2/c^2\right\}$. This indicates that, depending on the initial and boundary conditions will lead to spatial attenuation of the mechanical waves due to the radiation of the electromagnetic waves that accompany the mechanical waves. Interestingly, classical elasto-dynamic dispersion relations can be obtained also for $\left\{\ell = h,\ \ k_1^2 = \omega^2/c^2\right\}$.

In the above result we have $\left\{c = c_p,\ \ h = h_p\right\}$ for the dilatational waves and $\left\{c = c_s,\ \ h = h_s\right\}$ for the transverse waves. The imaginary wave numbers imply attenuated or evanescent waves which now depend on frequency and on the micro-inertial length *h*.

5. Comparison with experimental results

The dispersion relations can be utilized to obtain certain material properties by fitting available experimental dispersion curves: equations (3.1) and (3.6) for the acoustical modes and equations (3.12) and (3.16) for the optical modes. In case of known material properties the fitting should be direct and reasonably accurate. This is shown in **Figure 4** where we show the dispersion relations for (a) Si (diamond structure) and (b) $SrTiO_3$ (perovskite structure) and for (c) KTaO3 and (b) Ge for shear waves. The plots show the frequency ω versus the normalized wave number $0 \leq ka_0/\pi \leq 1$. The experimental results are: for Si from **Weber (1977)**, for $SrTiO_3$ from **Yamada and Shirane (1969)**, for $KTaO_3$ from **Sahin and Dost (1988)**, and for Ge from Weber (1974). The most complete set of data is available for Ge and $KTaO_3$. The set of obtainable parameters are shown in **Table 3**. Note that the parameter $(e_{44} - f_{12})$ as well as $(e_{11} - f_{11})$ can only be obtained as an absolute number.

Table 3 Typical material constants calculated from the experimental dispersion curves of Fig. 4 (shear).

Property	$SrTiO_3$ [100] 90 K	$KTaO_3$ [100] 39 K	Ge [111]	Si [111]
a_0 (nm)	0.391	0.399	0.566	0.543
$\rho(kg/m^3)$	5174	6970	5360	2330
$c_{44} = \mu$(GPa)	122	107	59.4	79.1
a (10^8 Nm^2/C^2)	2.12	0.355	75.3	103
$(b_{44} + b_{77})$ (10^{-9} Nm^4/C^2)	2.00	0.435	1.16	1.45
$(e_{44} - f_{12})$ (Nm/C=V)	− 10.0	6.00	(+/-) 8.80	(+/-) 11.0

Ω_s (THz)	1.46	4.79	9.00	15.5
c_s (m/s)	4856	3910	3538	5827
h_s (nm)	3.07	3.50	1.272	1.503
ℓ_s (nm)	2.36	1.66	0.00	0.00

6. Plane waves

Let us assume plane displacement waves (of direction $\vec{d}$) propagating with phase velocity c in a direction $\vec{p}$:

$$\vec{u} = f(\vec{x}\cdot\vec{p}-ct)\vec{d}$$
$$\vec{P} = g(\vec{x}\cdot\vec{p}-ct)\vec{d} \quad (6.1)$$

$\vec{d}, \vec{p}$ are unit vectors and $f(\vec{x}\cdot\vec{p}-ct)$, $g(\vec{x}\cdot\vec{p}-ct)$ are arbitrary functions of $(\vec{x}\cdot\vec{p}-ct)$. Without loss of generality, we will focus on plane problems (parallel to the $x_3 = 0$ plane) and decompose the fields according to the dilatation and deviatoric parts as in **Giannakopoulos and Rozakis (2020)**, in the absence of body forces and initial electric field):

$$u_1(x_1,x_2,t) = \frac{\partial\phi}{\partial x_1} + \frac{\partial H_3}{\partial x_2}$$
$$u_2(x_1,x_2,t) = \frac{\partial\phi}{\partial x_2} - \frac{\partial H_3}{\partial x_1} \quad (6.2)$$
$$u_3(x_1,x_2,t) = 0$$

with unknown potentials $\phi(x_1,x_2,t)$ and $H_3(x_1,x_2,t)$. Accordingly, the polarization vector is:

$$P_1(x_1,x_2,t)=\frac{\partial \chi}{\partial x_1}+\frac{\partial K_3}{\partial x_2}$$

$$P_2(x_1,x_2,t)=\frac{\partial \chi}{\partial x_2}-\frac{\partial K_3}{\partial x_1} \tag{6.3}$$

$$P_3(x_1,x_2,t)=0$$

with unknown potentials $\chi(x_1,x_2,t)$ and $K_3(x_1,x_2,t)$. The electric potential is $\Phi=\Phi(x_1,x_2,t)$. The mechanical dynamic equations (2.25) and (2.26) become:

$$\nabla^2\phi-\ell_p^2\nabla^4\phi=\frac{1}{c_p^2}\left(\ddot{\phi}-h_p^2\nabla^2\ddot{\phi}\right) \tag{6.4}$$

$$\nabla^2 H_3-\ell_s^2\nabla^4 H_3=\frac{1}{c_s^2}\left(\ddot{H}_3-h_s^2\nabla^2\ddot{H}_3\right) \tag{6.5}$$

The polarization equations (2.27) and (2.28) become:

$$\nabla^2\chi-\ell_p^2\nabla^4\chi=\frac{1}{c_p^2}\left(\frac{e_{11}-f_{11}}{a+\varepsilon_0^{-1}}\nabla^2\ddot{\phi}\right) \tag{6.6}$$

$$\nabla^2 K_3-\ell_s^2\nabla^4 K_3=\frac{1}{c_s^2}\left(\frac{e_{44}-f_{12}}{a}\nabla^2\ddot{H}_3\right) \tag{6.7}$$

In the above equations, $\nabla^2=\partial^2/\partial x_1^2+\partial^2/\partial x_2^2$ is the two-dimensional Laplacian operator, and $\nabla^4=\nabla^2\nabla^2=\partial^4/\partial x_1^4+2\partial^4/\partial x_1^2\partial x_1^2+\partial^4/\partial x_2^4$ is the two-dimensional biharmonic operator. When all micro-structural and micro-inertial lengths are zero, reduce to the plane stress classical elastodynamic equations, **Achenbach (1990)**.

Substituting (6.1) into (6.4) and (6.6) we obtain for $\vec{d}\cdot\vec{p}=\pm 1$ (motion parallel to the wave propagation, i.e. longitudinal wave, + forward and – backward),

$$\boxed{c^2=c_p^2\frac{\ell_p^2}{h_p^2}\le c_p^2} \tag{6.8}$$

$$g'-\ell_p^2 g'''=\pm c_p^2\frac{\ell_p^2}{h_p^2}\left(\frac{e_{11}-f_{11}}{a+\varepsilon_0^{-1}}\right)f''' \tag{6.9}$$

where $(\ )'$ denotes derivative with respect to $(\vec{\mathrm{x}}\cdot\vec{\mathrm{p}}-\mathrm{ct})$. For $\left(\vec{d}\times\vec{p}\right)_3=\pm 1$ (motion normal to the wave propagation, i.e. transverse or rotational wave + forward and – backward),

$$\boxed{c^2=c_s^2\frac{\ell_s^2}{h_s^2}\le c_s^2} \tag{6.10}$$

$$g'-\ell_s^2 g'''=\pm c_s^2\frac{\ell_s^2}{h_s^2}\left(\frac{e_{44}-f_{12}}{a}\right)f''' \tag{6.11}$$

Note that the longitudinal (6.8) and transverse (6.10) velocities of the plane waves were found to depend on the corresponding microstructural lengths and are less of equal to the classic plane wave velocities.

6.1 Time-harmonic plane waves

Let us now consider time-harmonic plane waves by letting the vectors $\vec{d},\vec{p}$ be either real or imaginary so that $\vec{d}\cdot\vec{p}=real$. The functions *f* and *g* particularize to:

$$\begin{aligned} f&=\mathrm{A}\exp[\mathrm{ik}(\vec{\mathrm{x}}\cdot\vec{\mathrm{p}}-\frac{\omega}{k}\mathrm{t})]\\ g&=B\exp[\mathrm{ik}(\vec{\mathrm{x}}\cdot\vec{\mathrm{p}}-\frac{\omega}{k}\mathrm{t})] \end{aligned} \tag{6.12}$$

where A and B are real or imaginary constants with $A\vec{d}=real, B\vec{d}=real$ and k the wave number (complex in general). Denote by $\omega=kc$ the circular frequency (real), related to a time period $2\pi/\omega$.

Replacing (6.12) in (6.4) and (6.5), we obtain:

$$\left(\frac{\omega}{k}\right)_p^2=c_p^2\left(\frac{1+\ell_p^2k^2}{1+h_p^2k^2}\right) \tag{6.13}$$

for the longitudinal waves and

$$\left(\frac{\omega}{k}\right)_s^2 = c_s^2\left(\frac{1+\ell_s^2 k^2}{1+h_s^2 k^2}\right) \tag{6.14}$$

for the transverse waves. These results are the same as (3.1) and (3.6).

Replacing (6.12) in (6.9) and (6.11), we obtain:

$$B\left(1+\ell_p^2 k^2\right) = \mp\left(\frac{e_{11}-f_{11}}{a+\varepsilon_0^{-1}}\right)A\omega^2 \tag{6.15}$$

which is the same as (3.12) for the longitudinal waves.

Replacing (6.12) in (6.10) and (6.12), we obtain:

$$B\left(1+\ell_s^2 k^2\right) = \mp\left(\frac{e_{44}-f_{12}}{a}\right)A\omega^2 \tag{6.16}$$

which is the same as (3.16) for the transverse waves.

7. Flexoelectric metamaterials

The previous analysis has been based on the assumption the dielectric susceptibility is positive $\chi > 0$, hence $a > 0$. This assumption seems to be true for all known homogeneous dielectrics. The positive value of susceptibility leads to the fact that the ratios of the microinertial to the microstructural lengths is greater than one, $h_s / \ell_s \geq 1, \quad h_p / \ell_p \geq 1$. This result stems from eqs. (2.30) and (2.31).

However, **Verlago (1968)** pointed out the possibility of negative electric susceptibility $\chi < 0$, hence $a < 0$, but it was realized that at the time there was no such materials, natural of artificial. In recent years, synthetic materials have appeared that show negative electric susceptibility and have been termed as *diaelectric metamaterials*, see for example **Koo (2015)**. Optical metamaterials can be considered as flexoelectric metamaterials which can be regarded as effective media with simultaneously negative electric permittivity and negative magnetic permeability and thus an effectively negative refractive index, **Lu et al (2009)**. In such cases, eqs. (2.30) and (2.31) indicate that $h_s / \ell_s < 1, \quad h_p / \ell_p < 1$. This possibility for flexoelectric materials was realized first by **Giannakopoulos and Zisis (2020)**. Other flexoelectric metamaterials can be composites of dielectric

matrix with aligned metal fibres (see for example related reviews **of Padilla et al (2006)** and **Smith et al (2004)**).

The first generation of optical negative index metamaterials were constructed from a printed (shadow mask/etching) circuit board material of fiber glass, with regular arrays of copper split-ring resonators (SRR) (see, for example, **Shelby et al.(2001)**). The SRR concept was originally introduced by **Pendry et al. (1999)**: the two metal micro-rings form the inductances and the two slits as well as the gap between the two rings form the capacitors, with the electric field being parallel to the SRR plane. Negative refractive index of metal–dielectric composites has been suggested by **Kildishev et al. (2006)**, with a simple structure consisting of a periodic array of identical gold strips. Clearly, it is not the scope of the present work to include all the research that has been carried out with respect to the field of composite optical metamaterials. It suffices to point that these composites include ever smaller metal particles in various dielectric matrices (mainly plastics), which are to be used in high-frequency applications.

The longitudinal (6.8) and transverse (6.10) velocities of the plane waves was found to depend on the corresponding microstructural lengths and are less than or equal to the classic plane wave velocities because the micro-inertial lengths are greater than or equal to the micro-structural length. The opposite effect is expected when we encounter flexoelectric metamaterials in which case the micro-inertial lengths are less than the micro-structural length.

Figure 5a shows the normalized plot of the mechanical modes, implied by eqs. (3.1) and (3.6) for the case of flexoelectric metamaterials $h_s / \ell_s \geq 1, \;\; h_p / \ell_p \geq 1$. **Figure 5b** shows the normalized plot of the optical modes, implied by eqs. (3.12) and (3.14). The normalized wave number is $\bar{\mathrm{k}} = \mathrm{k}h_{p,s}$. The suffix p,s denotes dilatational and shear part accordingly. The normalized frequency for the mechanical modes is $\bar{\omega} = \omega h_{p,s} / c_{p,s}$. The normalized frequency for the optical modes is $\bar{\omega} = \omega / \Omega_{p,s}$. Note the anomalous dispersion curves that appear (comparing with the results of **Fig.1)**.

Figure 6a shows the normalized *mechanical phase velocity* $\bar{\omega} / \bar{k}$, as a function of the normalized wave number $\bar{k}$ for the case of flexoelectric metamaterials. **Figure 6b** shows the normalized *optical phase velocity* $\bar{\omega} / \bar{k}$, as a function of the normalized wave number $\bar{k}$ for the case of flexoelectric metamaterials. **Figure 7a** shows the normalized *mechanical group velocity* $d\bar{\omega} / \mathrm{d}\bar{\mathrm{k}}$, as a function of the normalized wave number $\bar{k}$. **Figure 7b** shows the normalized *optical group velocity* $d\bar{\omega} / d\bar{k}$, as a function of the normalized wave number $\bar{k}$.

Regarding the mechanical phase velocity, we observe the analogy with the phase velocity that is encountered in the dynamic behavior of a Zener type (standard) viscoelastic model, **Carcione (2007)**. Viscoelasticity shows anomalous dispersion curves like the ones shown by the flexoelectric metamaterials. The phase velocity $c_{ph} = \omega / k$ for the simple shear wave traveling in the standard viscoelastic solid, normalized by the shear wave speed c_s is given by (**Carcione (2007)**)

$$\boxed{\frac{(\omega / \mathrm{k})}{c_s} = \mathrm{Re}\left[\sqrt{\frac{1+i\omega\tau_\varepsilon}{1+i\omega\tau_\sigma}}\right]} \tag{7.1}$$

where $i = \sqrt{-1}$, ω is the frequency, k is the wave length and $\tau_\varepsilon \geq \tau_\sigma > 0$ are the relaxation times. It is easy to show that the analogy with eq. (3.7) requires

$$\boxed{\frac{\ell_s}{h_s} = \frac{\tau_\sigma}{\tau_\varepsilon} \geq 1} \tag{7.2}$$

Therefore the flexoelectric metamaterial model is analogous to the Zener viscoelastic model, with eq. (7.2) describing the parameter equivalence.

8. Conclusions

We have extended our flexoelectric analysis an investigated the dispersion relations and found that for each, dilatational and shear, mechanical types of waves, two coupled branches appear: an acoustic and an optical one that approximate well the experimental results for many flexoelectric materials. The dispersion relations are affected strongly by the two microstructural lengths. These dispersion relations are not expected in classical elasto-dynamics where the absence of internal lengths leads to no dispersion relations. Moreover we have investigated the role of the group velocity as a velocity of energy transport and showed that it also has dispersive character, in contrast to the classic case that shows no dispersion (group velocities are identical to the phase velocities). A notable similarity with the classic elasto-dynamics is that the plane waves are also partitioned to longitudinal and transverse waves with distinct dispersion relations and group velocities. The present results fall back to the classic results in absence of the flexoelectric related microlengths. An optical branch of the dispersion relation appears due to the polarization field that follows the mechanical

field. The longitudinal and transverse velocities of the plane waves was found to depend on the corresponding microstructural lengths and are less than or equal to the classic plane wave velocities.

Dispersion relations that look like the ones found in this work resemble dispersion of structural wave guides like circular cylinders and plates when investigated by classic elasto-dynamics. In the later cases the characteristic lengths are macroscopic dimensions of waveguides like the cylinder radius and the plate thickness. It should be made clear that the present theory should investigate such wave guides and quantify the competition between the macroscopic length scales with the present microscopic length scales

The dispersion relations were found to correlate well with available experimental results where the acoustic branches are always accompanied with the optical branches. These branches were found with the present models and although they may not be fully adequate, they serve well as good approximations.

An interesting analogy has been established between viscoelastic models and flexoelectric metamaterials. Flexoelectic metamaterials accept negative sign of the dielectic constant (accompanied by a similar change of sign of the magnetic permeability) and could lead to anomalous dispersion curves, just as the ones predicted by the vicoelastic models. The analogy is based on the ratio of the microstructural vs the microinertia lengths that correspond to the characteristic times of the viscoelasticity (creep/relaxation).

The results are important for all dielectrics such as ceramics, ice, perovskites and polymers that exhibit strong flexoelectric effect, often uncoupled from piezoelectricity (centrosymmetric materials). However, the results also apply to nano-composite and atomistic models that can be approached in the context of couple stress elasticity. In such cases, the origin of the micro-structural and micro-inertial lengths is very different that the one proposed in this work.

Appendix. The group velocity as an energy transport velocity

In this **Appendix** we show that the mechanical group velocities (eq. (3.26)) are the velocities of the transfer of the time average of the power per unit area to the twice the time average of the kinetic

energy across the plane of a time-harmonic plane wave (longitudinal and transverse) that travel inside the body. The time average over a period of the power per unit area of the advancing plane is:

$$\left\langle \wp \right\rangle = -\frac{\omega}{2\pi}\int_0^{2\pi/\omega}\left(t_i \dot{u}_i + r_i p_j \frac{\partial \dot{u}_i}{\partial x_j} + p_i E_{ij} \dot{P}_j \right) dt \tag{A.1}$$

where

$$t_i = \sigma_{ij} p_j - \tau_{kji,k} p_j + (D_l n_l) p_j p_k \tau_{kji} - D_j (\tau_{kji} p_k),\ D_j = (\delta_{jk} - p_j p_k)\partial / \partial x_k \tag{A.2}$$

$$r_i = \tau_{kji} p_k p_j \tag{A.3}$$

$$E_{ij} = b_{ijkl} P_{l,k} + e_{ijkl} \varepsilon_{kl} + b_{ij}^0 \tag{A.4}$$

The corresponding time average of the internal energy density and kinetic energy density is $\langle W \rangle + \langle T \rangle = 2\langle T \rangle$ in the absence of energy dissipation. The time average of the kinetic energy is:

$$\left\langle T \right\rangle = \frac{\omega}{2\pi}\int_0^{2\pi/\omega}\left(\frac{1}{2}\rho \dot{u}_i \dot{u}_i \right) dt \tag{A.5}$$

Then, the velocity of the energy transport by plane time-harmonic waves c_e is defined as:

$$\left\langle \wp \right\rangle = 2\left\langle T \right\rangle c_e \tag{A.6}$$

Without loss of generality we utilize the results of Section 6.1 and replace them in the above equations. After a lengthy but straightforward algebra, we obtain for the longitudinal waves:

$$c_e = c_p \left(1+\ell_p^2 k^2\right)^{1/2}\left(1+h_p^2 k^2\right)^{-1/2} + c_p\left(\ell_p^2 k^2 - h_p^2 k^2\right)\left(1+\ell_p^2 k^2\right)^{-1/2}\left(1+h_p^2 k^2\right)^{-3/2} \tag{A.7}$$

and

$$c_e = c_s \left(1+\ell_s^2 k^2\right)^{1/2}\left(1+h_s^2 k^2\right)^{-1/2} + c_s\left(\ell_s^2 k^2 - h_s^2 k^2\right)\left(1+\ell_s^2 k^2\right)^{-1/2}\left(1+h_s^2 k^2\right)^{-3/2} \tag{A.8}$$

for the tangential waves. These results are identical with the group velocity results found in eqs. (3.3) and (3.8) respectively. Thus, for the mechanical dispersion relations

$$c_e = \left(\frac{d\omega}{dk}\right)_{p,s} \tag{A.9}$$

References

Achenbach J. D. (1990) Wave Propagation in Elastic Solids. North-Holland Publications.

Askar A., Lee P.C.Y. and Cakmak A.S. (1970) Lattice-dynamics approach to the theory of elastic dielectrics with polarization gradient. Physical Review B 1: 3525-3537.

Axe J.D., Harado J. and Shirane G. (1970) Anomalous acoustic dispersion in centrosymmetric crystals with soft optic phonons. Physical Review B, 1: 1227-1234.

Barrett J.H. (1952) Dielectric constant in perovskite type crystals. Phys. Review 86: 118-120.

Bleusten J.L. and Stanley R.M. (1970) A dynamical theory of torsion. Int. J. Solids and Structures 6: 569-586.

Born M. and Wolf E. (1999) Principles of Optics. 7th edition. Cambridge University Press.

Brillouin L. (1946) Wave Propagation in Periodic Structures. New York, McGraw-Hill.

Carcione J. M. (2007) Wave Fields in Real Media: Wave Propagation in Anisotropic, Anelastic, Porous and Electromagnetic Media: Third Edition Chapter 2. Viscoelasticity and wave propagation pp. 51-95. Elsevier

Gavardinas I.D., Giannakopoulos A.E. and Zisis Th. (2018) A von Karman plate analogue for solving anti-plane problems in couple stress and dipolar gradient elasticity. Int. J. Solids Structures 148-149: 169-180.

Giannakopoulos A.E. and Rosakis A.J. (2020) Dynamics of flexoelectric materials: Subsonic, intersonic and supersonic ruptures and Mach cone formation. Journal of Applied Mechanics ASME 87: 061004-1/9.

Giannakopoulos A.E. and Zisis Th. (2019) Uniformly moving screw dislocation in flexoelectric materials. European Journal of Mechanics / A Solids 78-149: 103843.

Giannakopoulos A.E. and Zisis Th. (2020) Uniformly moving antiplane cracks in flexoelectric materials. European Journal of Mechanics / A Solids 85-104136.

Giannakopoulos A.E. and Zisis Th. (2021) Steady-state antiplane crack considering the flexoelectric effect: surface waves and flexoelectric metamaterials. Arch. Appl. Mech. 10.1007.

Hu S. and Shen S. (2010) variational principles and governing equations in nano-dielectrics with the flexoelectric effect. Sci. China Physics, Mech. Astron. 53: 1497-1504.

Gugliemi A.V., Tsegmed B., Potapov A.S., Kultima J. and Raita T. (2006) Seismomagnetic signals from the strong Sumatra Earthquake. Izvestia, Physics of the Solid earth 42: 921-927.

Gouriotis P.A. and Georgiadis H.G. (2017) Torsional and SH waves in an isotropic and homogeneous elastic half-space characterized by the Toupin-Mindlin gradient theory. Int. J. Solids Structures 62: 217-228.

Harado J., Axe J.D. and Shirane G. (1971) Neutron-scattering study of soft modes in cubic BaTiO3. Physical Review B, 4:155-62.

Huller A. (1969) Soft phonon dispersion in BaTiO3 Z. Physik 220: 145-158.

Jackson J.D. (1975) Classical Electrodynamics, John Willey & Sons, New York.

Kildishev, A.V., Cai, W., Chettiar, U.K., Yuan, H.K., Sarychev, A.K., Drachev, V.P., Shalaev, V.M.: Negative refractive index in optics of metal–dielectric composites. JOSA B 23(3), 423–433 (2006).

Koo J.H. (2015) Negative electric susceptibility and magnetism from translational invariance and rotational invariance. Journal of Magnetism and Magnetic Materials 375: 106-110.

Krichen S. and Sharma P. (2016) Flexoelectricity: A perspective on an unusual electromechanical coupling. J. Appl. Mech. 83.030801.

Kittel C. (1971) Introduction to Solid State Physics, Wiley, New York.

Lu, M.H., Feng, L., Chen, Y.F.: Phononic crystals and acoustic metamaterials. Mater. Today 12(12), 34–42 (2009).

Maranganti R., Sharma N.D. and Sharma P. (2006) Electromechanical coupling in non-piezoelectric materials due to nanoscale nonlocal size effects: Green's functions and embedded inclusions. Phys. Review B74.014110. Erratum: Piezoelectric thin-film super-lattices without using piezoelectric materials [J. Appl. Phys. 108, 024304 (2010)] N. D. Sharma, C. Landis, and P. Sharma.

Mindlin R.D. (1963) Micro-structure in linear elasticity. Arch. Rational Mech. Anal. 16: 51-78.

Mindlin R.D. (1968) Polarization gradient in elastic dielectric. Int. J. Solids Structures, 4:637-642.

Mindlin R.D. (1969) Continuum and lattice theories of influence of electromechanical coupling on capacitance of thin dielectric films. Int. J. Solids Structures 5: 1197-1208.

Mindlin R.D. and McNiven H.D. (1960) Axially symmetric waves in elastic rods. Journal of Applied Mechanics 145-151.

Padilla W.J., Basov D. N. and Smith D.R. (2006) Negative refractive index metamaterials. Materials Today 9: 28-35.

Pendry, J.B., Holden, A.J., Robbins, D.J., Stewart, W.J. (1999) Magnetism from conductors and enhanced nonlinear phenomena. IEEE Trans. Microwave Theory Tech. 47(11): 2075–2084.

Pochhammer L. (1876) Uber die fortpflansungsgesehwindigkeiten schwingungen in einem unbegrensten isotropen kreiscylinder. Zeitschrift fur Mathematik 81: 324-336.

Qu Y., Jin F. and Yang J. (2021a) Flexoelectric effects in second-order extension of rods. Mech. Res. Communications 103625.

Qu Y., Jin F. and Yang J. (2021b) Torsion of a flexoelectric semiconductor rod with a rectangular cross section. Arch. Appl. Mech. Doi.org/10.1007/s00419-020-01867-0.

Shahin E. and Dost S. (1988) A strain-gradient theory of elastic dielectrics with dispersion. Int. J. Engng. Sci. 26: 1231-1245.

Shelby, R.A., Smith, D.R., Nemat-Nasser, S.C., Schultz, S.: Microwave transmission through a two-dimensional, isotropic, left-handed metamaterial. Appl. Phys. Lett. 78(4), 489–491 (2001).

Shirane G., Axe J.D., Harada J. and Remeika J.P. (1970) Soft ferroelectric modes in lead titanate. Physical Review B, 2: 155-159.

Shu L., Wei X., Pang T., Yao X. and Wang C. (2011) Symmetry of flexoelectric coefficients in crystalline medium. Journal of Applied Physics, 110: 104106.

Smith D.R., Pendry J.B and Wiltshire M.C.K. (2004) Metamaterials and negative refractive index. Science 305: 788-792.

Tagantsev A.K. (1991) Electric polarization in crystals and its response to thermal and elastic perturbations. Phase Transitions 35: 119-203.

Toupin R.A. (1956) The elastic dielectric. J. Ration. Mech. Anal. 5: 849-915.

Veselago V.G. (1968) The electrodynamics of substances with simultaneously negative values of ε and μ. Soviet Physics 10: 509-514.

Wang B., Gu Y., Zhang S. and Chen L.-Q. (2019) Flexoelectricity in solids: Progress, challenges and perspectives. Progress in Materials Sciences 100570.

Weber W. (1974) New bond-charge model for the lattice dynamics of diamond-type semiconductors. Physical Review Letters 33: 371-374.

Weber, W.: Adiabatic bond charge model for the phonons in diamond, Si, Ge, and α-Sn. Phys. Rev. B 15, 4789–4803 (1977).

Yamada I., Masuda K. and Mizutani (1989) Electromagnetic and acoustic emission associated with rock fracture. Physics of the Earth and Plenary Interiors 57: 157-168.

Yamada, Y., Shirane, G.: Newton scattering and nature of the soft optical phonon in SrTiO3. J. Phys. Soc. Jpn. 26, 396–403 (1969).

Yudin P.V. and Tagantsev A.K. (2013) Fundamentals of flexoelectricity in solids. Nanotechnology 24: 43001.

Zubko P., Catalan G., Buckley A., Welch P.R.L. and Scot J.F. (2008) Strain gradient induced polarization in $StrO_3$ single crystals. Phys. Rev. Letters 99: 167601.

Figures

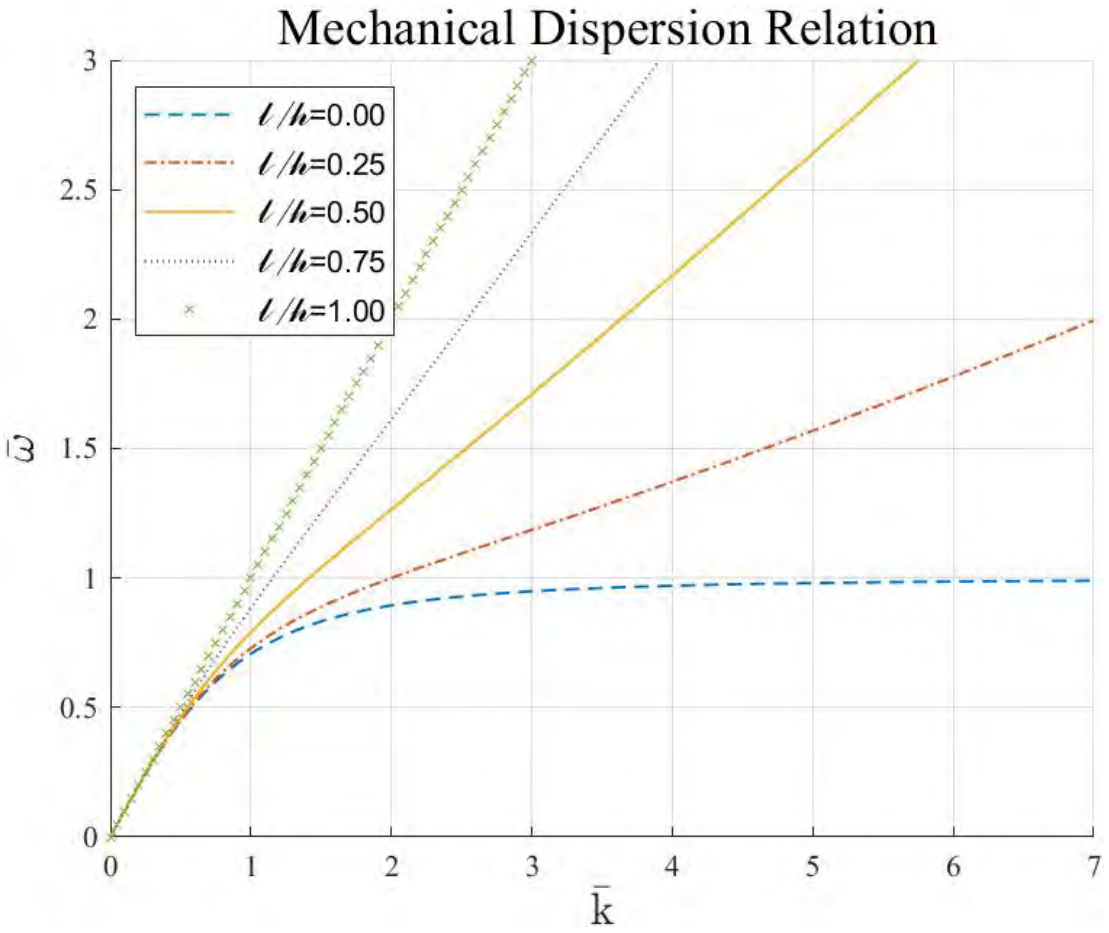

Figure 1a Normalized plot of the mechanical modes, implied by eqs. (3.1) and (3.6). The normalized frequency is $\bar{\omega} = \omega h_{p,s} / c_{p,s}$ and the normalized wave number is $\bar{k} = k h_{p,s}$. The suffix p,s denote dilatational and shear part.

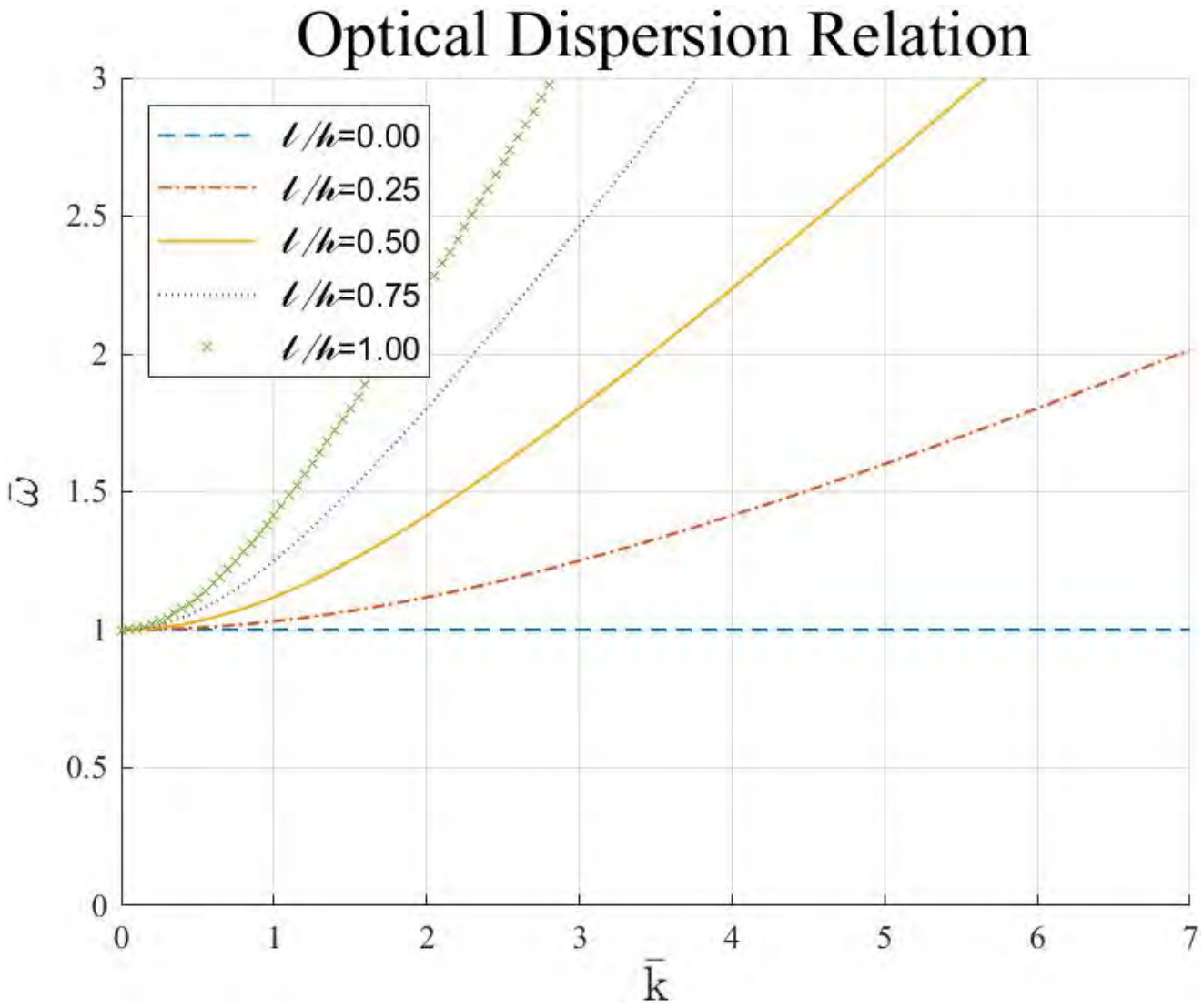

Figure 1b Normalized plot of the optical modes, implied by eqs. (3.12) and (3.14). The normalized frequency is $\bar{\omega} = \omega / \Omega_{p,s}$ and the normalized wave number is $\bar{\mathrm{k}} = \mathrm{k h}_{p,s}$. The suffix p,s denote dilatational and shear part.

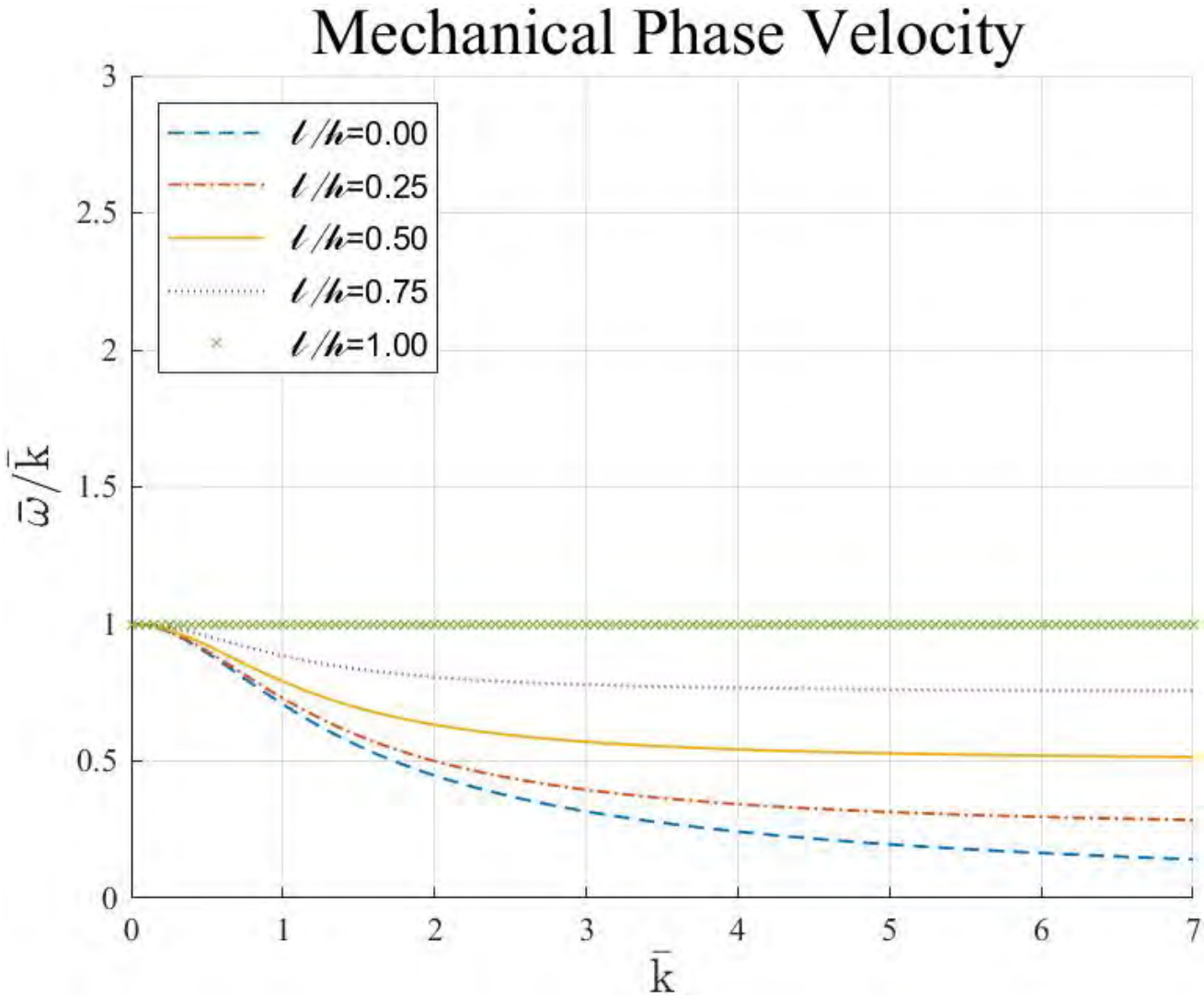

Figure 2a Normalized *mechanical phase velocity* $\bar{\omega}/\bar{k}$, as a function of the normalized wave number $\bar{k}$. The normalization is as in Fig. 1.

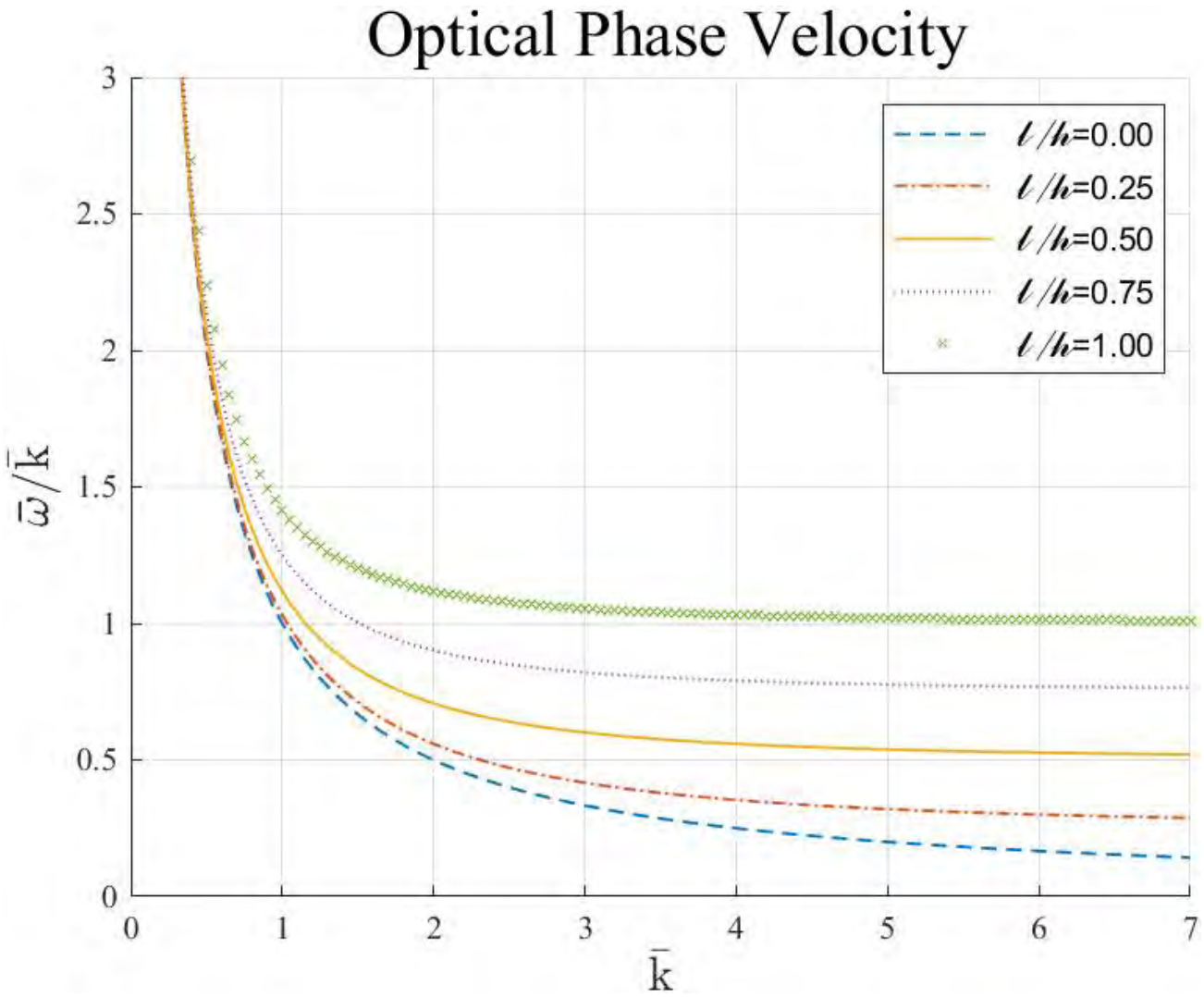

Figure 2b Normalized *optical phase velocity* $\bar{\omega}/\bar{k}$, as a function of the normalized wave number $\bar{k}$. The normalization is as in Fig. 1.

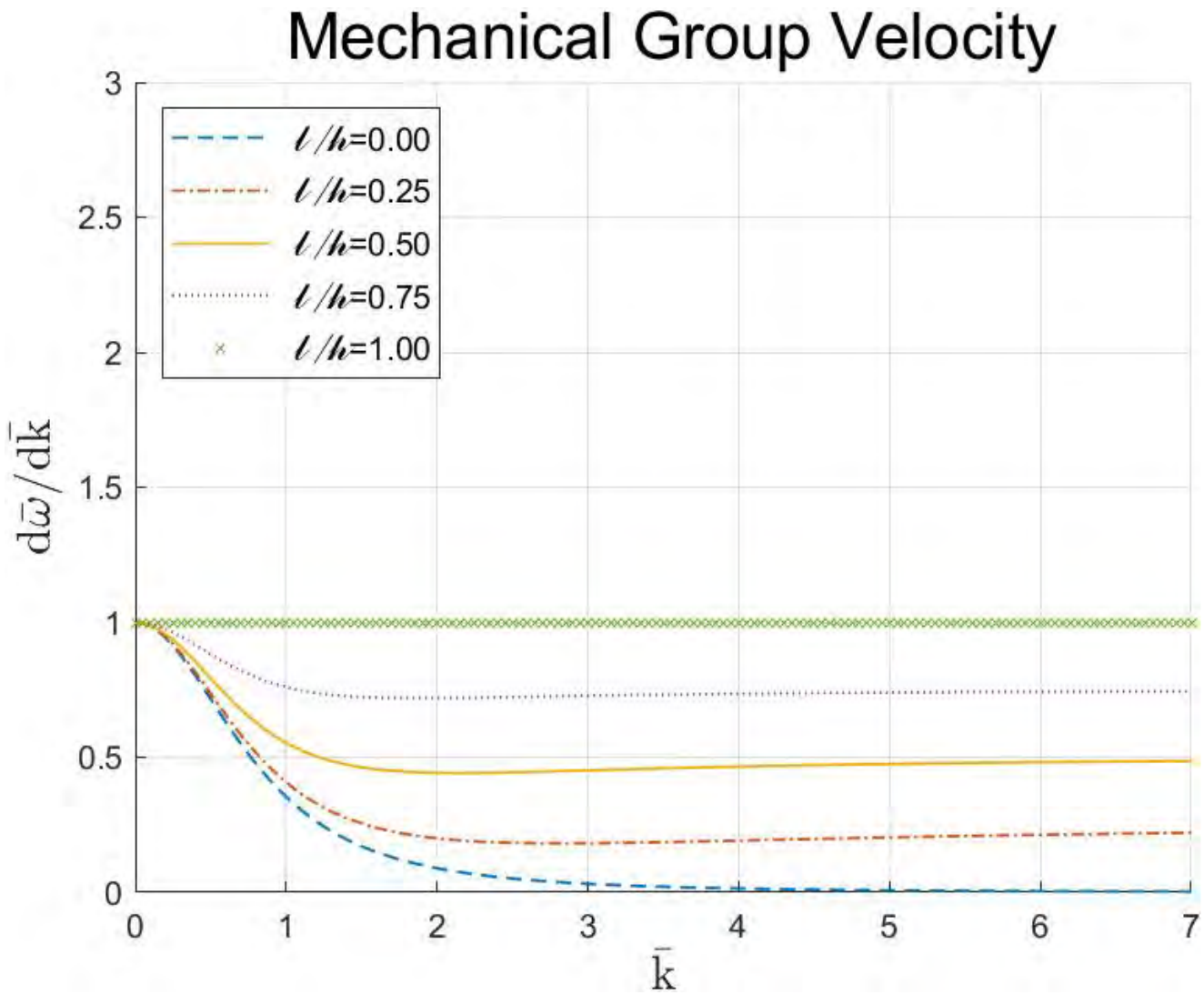

Figure 3a Normalized *mechanical group velocity* $d\bar{\omega}/\mathrm{d}\bar{\mathrm{k}}$, as a function of the normalized wave number $\bar{k}$. The normalization is as in Fig. 1.

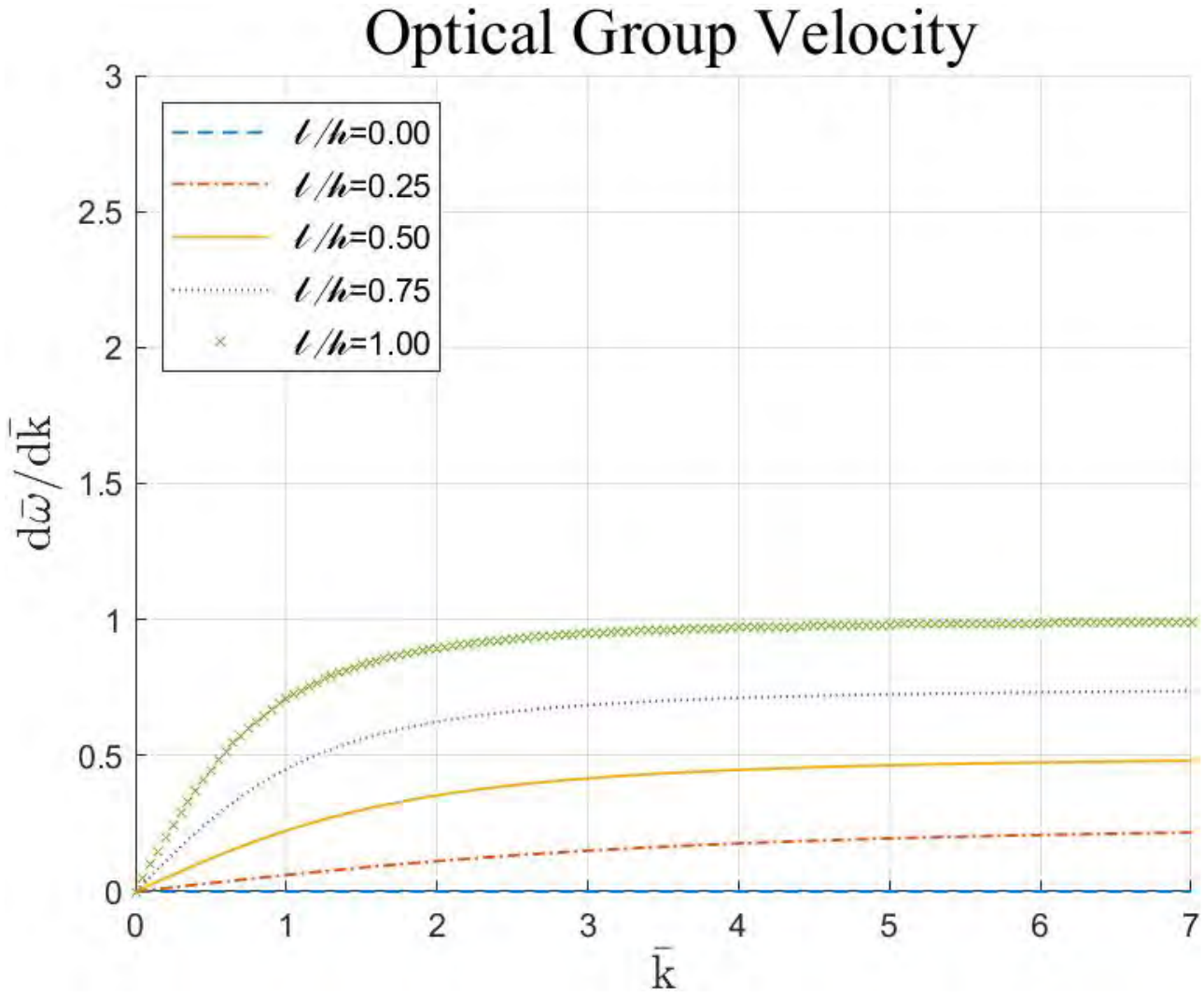

Figure 3b Normalized *optical group velocity* $d\bar{\omega}/d\bar{k}$, as a function of the normalized wave number $\bar{k}$.

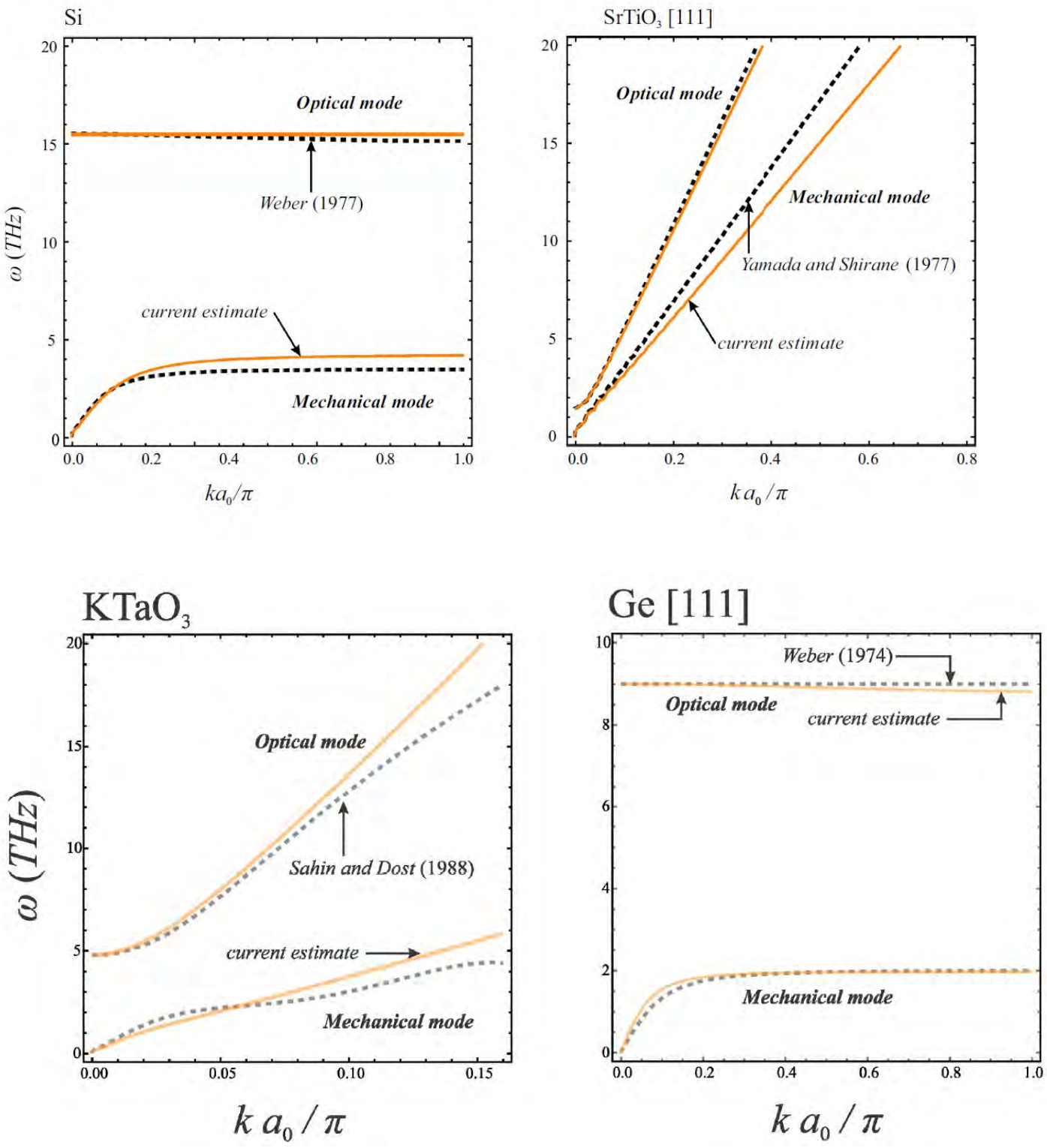

Figure 4 The dispersion relations for (a) Si (diamond structure) and (b) $SrTiO_3$ (perovskite structure) and for (c) KTaO3 and (b) Ge for shear waves. The plots show the frequency ω versus the normalized wave number $0 \leq ka_0/\pi \leq 1$. The experimental results are: for Si from Weber (1977), for $SrTiO_3$ ([111] shear) from Yamada and Shirane (1969), for $KTaO_3$ from Sahin and Dost (1988), and for Ge from Weber (1974).

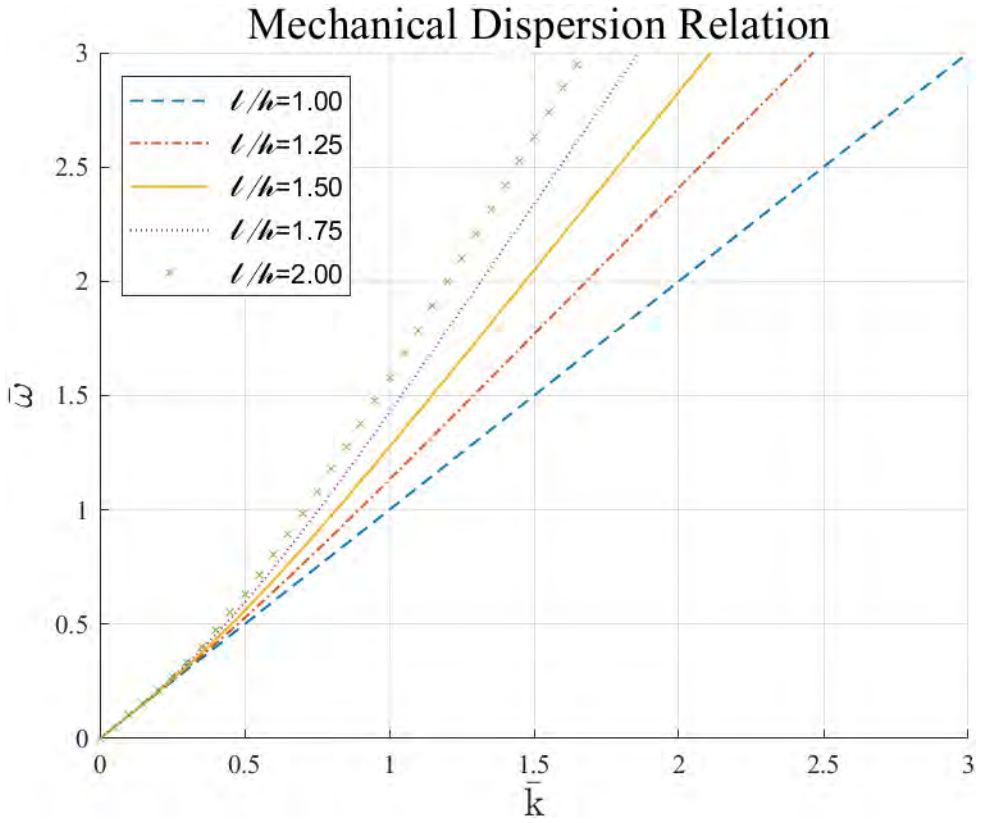

Figure 5a Normalized plot of the mechanical modes, implied by eqs. (3.1) and (3.6) for the case of flexoelectric metamaterials $h_s / \ell_s \geq 1$, $h_p / \ell_p \geq 1$. The normalized frequency is $\bar{\omega} = \omega h_{p,s} / c_{p,s}$ and the normalized wave number is $\bar{\mathrm{k}} = \mathrm{k} h_{p,s}$. The suffix p,s denote dilatational and shear part.

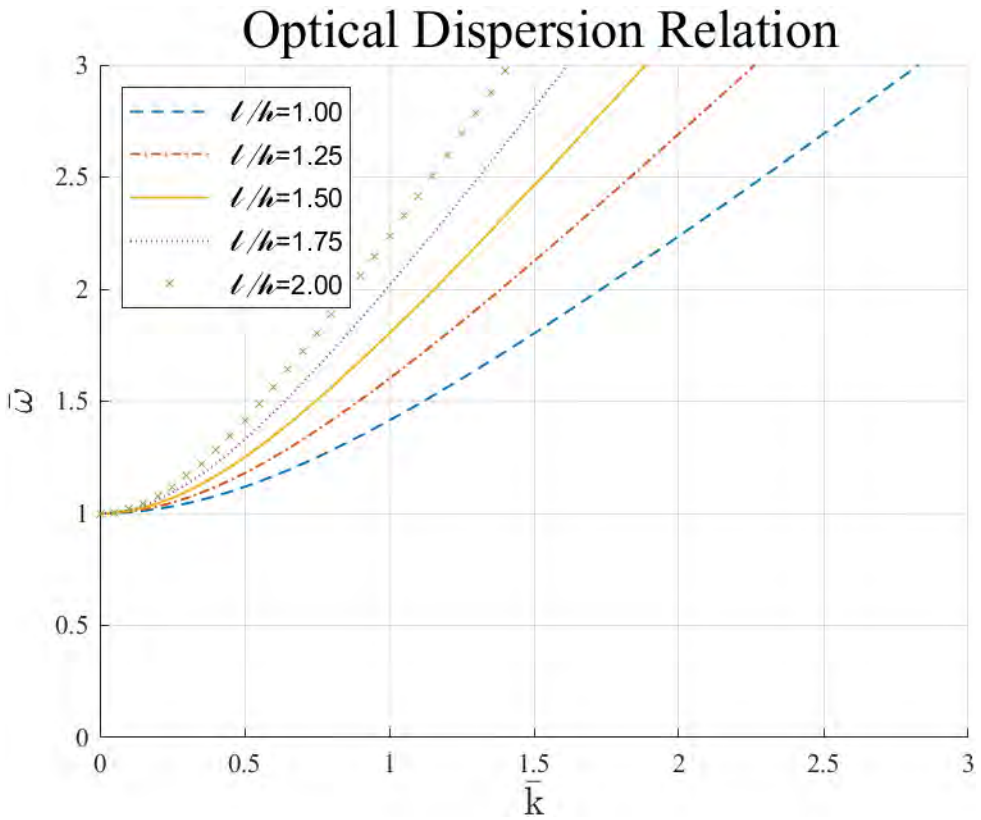

Figure 5b Normalized plot of the optical modes, implied by eqs. (3.12) and (3.14) for the case of flexoelectric metamaterials $h_s / \ell_s \geq 1, \;\; h_p / \ell_p \geq 1$. The normalized frequency is $\bar{\omega} = \omega / \Omega_{p,s}$ and the normalized wave number is $\bar{\mathrm{k}} = \mathrm{k} h_{p,s}$. The suffix p,s denote dilatational and shear part.

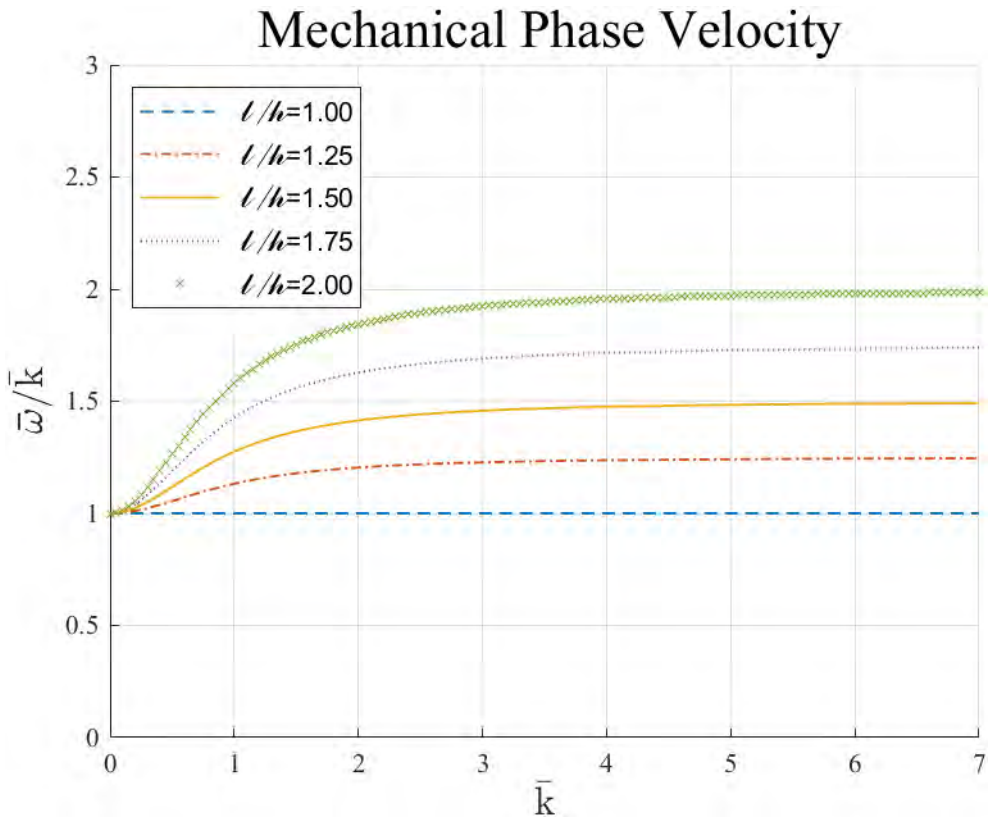

Figure 6a Normalized *mechanical phase velocity* $\bar{\omega}/\bar{k}$, as a function of the normalized wave number $\bar{k}$ for the case of flexoelectric metamaterials $h_s/\ell_s \geq 1$, $h_p/\ell_p \geq 1$. The normalization is as in Fig. 4.

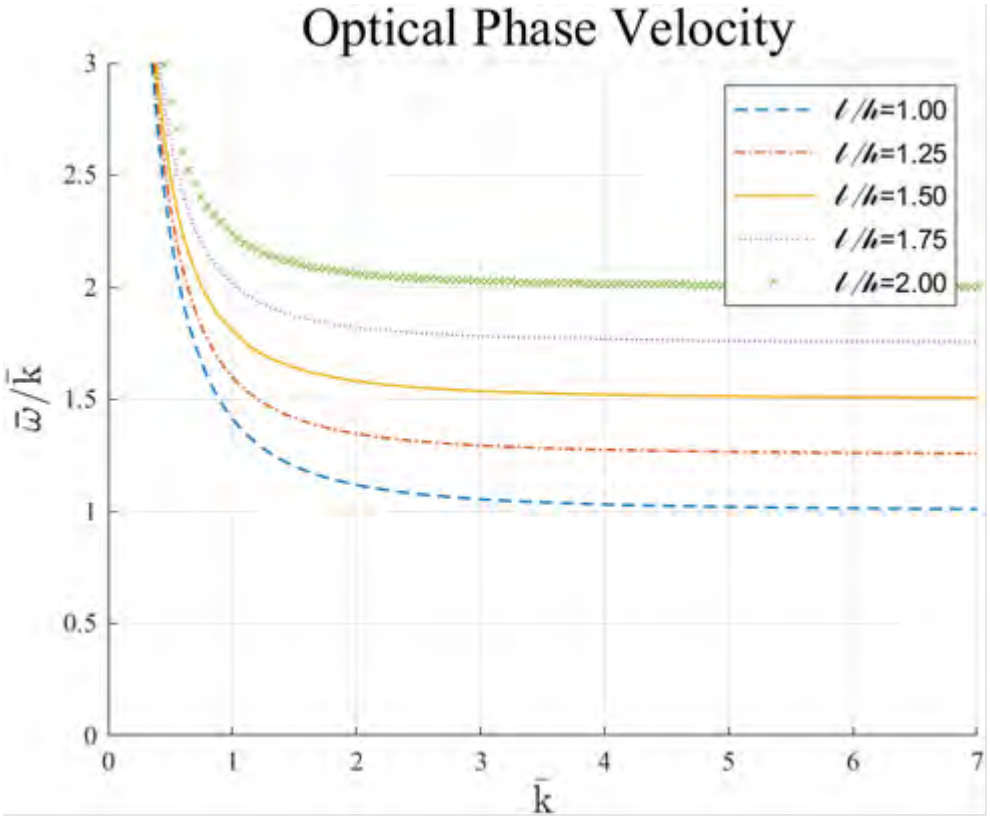

Figure 6b Normalized *optical phase velocity* $\bar{\omega}/\bar{k}$, as a function of the normalized wave number $\bar{k}$ for the case of flexoelectric metamaterials $h_s/\ell_s \geq 1$, $h_p/\ell_p \geq 1$. The normalization is as in Fig. 4.

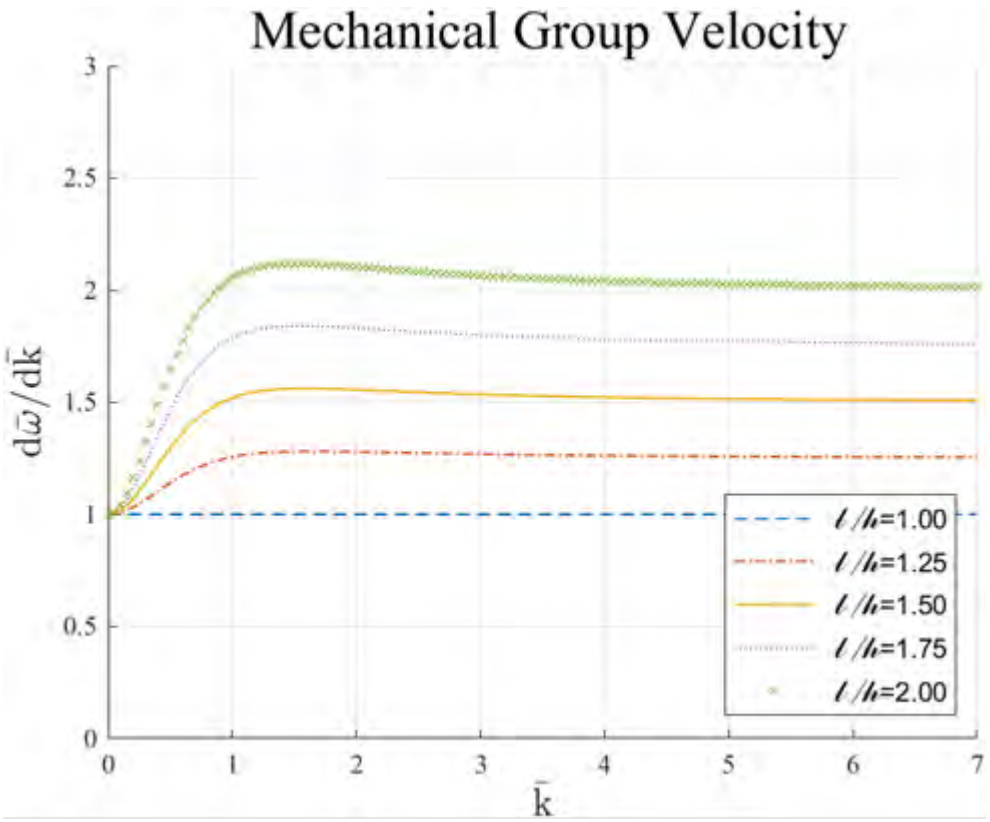

Figure 7a Normalized *mechanical group velocity* $d\bar{\omega}/\mathrm{d}\bar{\mathrm{k}}$, as a function of the normalized wave number $\bar{k}$ for the case of flexoelectric metamaterials $h_s/\ell_s \geq 1$, $h_p/\ell_p \geq 1$. The normalization is as in Fig. 4.

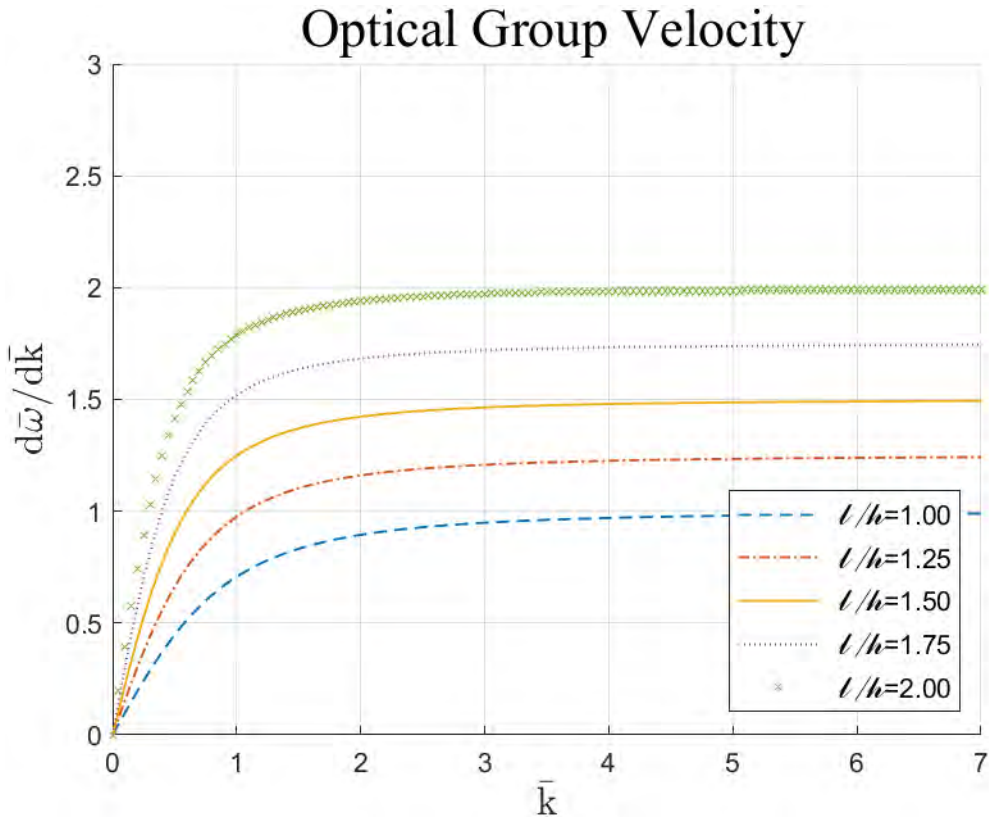

Figure 7b Normalized *optical group velocity* $d\bar{\omega}/d\bar{k}$, as a function of the normalized wave number $\bar{k}$ for the case of flexoelectric metamaterials $h_s/\ell_s \geq 1$, $h_p/\ell_p \geq 1$. The normalization is as in Fig. 4.